Food Hydrocolloids 176 (2026) 112581

Contents lists available at ScienceDirect

Food Hydrocolloids

journal homepage: www.elsevier.com/locate/foodhyd

Molecular basis of changes in pasting and rheological properties of starches physically modified by microwave radiation

Raúl Ricardo Mauro [a,b,c], Zhihang Li [c], Andreas Blennow [d], Ainhoa Vicente [a,b], Felicidad Ronda [a,b,*]

[a] Department of Agriculture and Forestry Engineering, Food Technology, College of Agricultural and Forestry Engineering, University of Valladolid, Spain
[b] Research Institute on Bioeconomy - BioEcoUVa, PROCEREALtech Group, University of Valladolid, Spain
[c] Department of Plant and Environmental Sciences, University of Copenhagen, DK-1871, Frederiksberg C, Denmark
[d] School of Food Science and Technology, Jiangnan University, Wuxi, Jiangsu, 214122, China

ARTICLE INFO

Keywords:
Microwave-assisted hydrothermal treatment
Starch fine structure
Pasting properties
Viscoelastic properties

ABSTRACT

This study investigates the effects of controlled microwave treatment (100 °C, 25% moisture, 30 min) on the molecular and rheological properties of pure starches (normal and waxy maize, normal and waxy rice, wheat, potato and tapioca). Structural changes were assessed through high-performance anion exchange chromatography with pulsed amperometric detection (HPAEC/PAD) to resolve amylopectin chain-length distributions, and size-exclusion chromatography with multi-angle light scattering, differential refractive index, and viscometric multi-detection (SEC/MALS-dRI-Visco) to determine amylose and amylopectin molecular parameters for both debranched and whole molecules. The impact of these changes on the pasting properties of starches and the viscoelasticity of their gels was established. Microwave treatment induced source-specific responses. Waxy starches showed increases in very short amylopectin chains and molecular degradation, with minimal rheological impact due to their low viscometric profile. Potato starch experienced the most pronounced rheological modifications despite minimal molecular degradation, suggesting supramolecular reorganisation, supported by an increase in amylopectin intrinsic viscosity. Wheat and tapioca starches exhibited moderate structural changes and enhanced gel stability, attributed to an increase of fractions comparable in size to long amylopectin chains. Rice starches displayed similar pasting and rheological responses, having amylopectin fine structure a predominant role, while the absence of amylose in waxy rice favoured greater amylopectin hydrolysis. Correlation analyses linked amylose short/medium chains to parameters related to stronger and firmer gels. In contrast, short amylopectin chains correlated with weaker gels. These findings offer mechanistic insight into the potential of controlled microwave processing to tailor starch functionality in food systems.

1. Introduction

Microwave treatment has emerged as an effective method for starch modification, enabling rapid and uniform structural and functional changes, thereby offering greater efficiency compared to other conventional thermal methods (Zhao et al., 2024). Numerous studies have documented that microwave treatment significantly alters starch pasting and rheological properties. However, these effects are highly dependent on multiple factors, as starch functionality is governed by its molecular and supramolecular architecture. This architecture is determined by amylose content and the fine structure and organisation of amylopectin, which are in turn influenced by botanical origin—reflecting genetic background and growth environment—as well as by starch variety and the specific thermal treatment applied. In rice starch, microwave treatment has been reported to increase final viscosity and setback, along with a decrease in loss tangent, indicating a higher proportion of elastic components within the gel matrix (Zhong, Xiang, Zhao, et al., 2020). Similarly, research on rice flour demonstrated increases across all pasting viscosities as well as in the elastic and viscous moduli, reflecting the formation of a more resilient and elastic gel network (Zhong, Xiang, Chen, et al., 2020). Effects on maize starches, appear more variable For waxy maize starch, microwave treatment reduced the

* Corresponding author. Department of Agriculture and Forestry Engineering, Food Technology, College of Agricultural and Forestry Engineering, University of Valladolid, Spain.
E-mail address: mfronda@uva.es (F. Ronda).

https://doi.org/10.1016/j.foodhyd.2026.112581
Received 9 January 2026; Received in revised form 8 February 2026; Accepted 18 February 2026
Available online 18 February 2026

proportion of A-chains, with a degree of polymerisation (DP) between 6 and 12 glucose units, while increasing B1 (DP 13-24), B2 (DP 25-36) and B3 (DP > 36) chains, accompanied by elevated pasting temperatures and an overall reduction in viscosities. These changes suggest diminished shear resistance and retrogradation tendency (Yang et al., 2017). A comprehensive study on maize starches with varying amylose contents found that treatment power exerted a greater influence than duration, with degradation of medium-length chains (DP 8–24), formation of both short and long chains, and reduced viscosities except for high-amylose starches, which exhibited greater stability and functional improvements (Tian et al., 2023). Tapioca starch subjected to microwave treatment showed decreased peak, final, trough, and setback viscosities, alongside increased pasting temperature and breakdown viscosity, indicative of enhanced granule swelling resistance and integrity (Oyeyinka et al., 2021).

Despite these advances, most studies focus on a single starch source at a time, lacking systematic comparisons across species under uniform treatment conditions. Moreover, many investigations employ fixed and continuous microwave power without strict control of temperature and moisture, introducing variability that complicates attributing observed effects specifically to the electromagnetic field versus thermal components of the treatment. Such control is critical, given that subtle differences in amylopectin fine structure can cause significant variations in gel formation and mechanical behaviour (Bertoft et al., 2016). Recent work with microwave-treated flours or grains under tightly controlled conditions demonstrated that gelatinisation or dehydration can be avoided, preserving structural integrity (Calix-Rivera et al., 2023; Vicente, Villanueva, et al., 2025).

In this context, the present study proposes an alternative approach involving microwave treatment at a constant temperature (~100 °C), achieved through intermittent on/off cycles within a hermetic system with initial controlled moisture set at 25%. This method was applied directly to isolated starches to exclude interference from other flour constituents such as proteins, lipids, or fibres. Seven starch sources from diverse species and with varying characteristics (normal rice, waxy rice, normal maize, waxy maize, wheat, potato, and tapioca) were included to enable a comprehensive comparison of treatment effects across different granular morphologies and amylose/amylopectin ratios. These starches represent a range of the most industrially relevant food starches.

To capture structural modifications at different levels of molecular organisation, High-Performance Anion-Exchange Chromatography with Pulsed Amperometric Detection (HPAEC/PAD) and Size-Exclusion Chromatography with multi-angle light scattering, differential refractive index, and viscometric multi-detection (SEC/MALS-dRI-Visco) were employed as complementary techniques. HPAEC/PAD was used to obtain comparative amylopectin chain-length profiles focusing on relative changes in the most abundant low- and intermediate-DP chains, while recognising its limited sensitivity towards high-DP fractions (Wong & Jane, 1995). SEC/MALS-dRI-Visco provided complementary molecular information, including amylose characterisation and size parameters of whole starch molecules. This integrated analytical approach enabled linking molecular changes to pasting and rheological behaviour, providing clear insight into how microwave-induced modifications under controlled thermal conditions affect starch functionality, with potential applications in designing food products with tailored textures and improved technological performance.

2. Material and methods

2.1. Samples

Seven types of starches were selected: normal maize, waxy maize, wheat, potato, and tapioca were manufactured by Cargill Inc. (Minneapolis, MN, USA) and supplied by Brenntag Química S.A.U. (Dos Hermanas, Seville, Spain). Normal and waxy rice starches (BENEO GmbH, Mannheim, Germany) were purchased from Ferrer Alimentación (Barcelona, Spain). All starches had a purity of more than 99 % on a dry basis.

2.2. Microwave treatment

The native starches were subjected to microwave treatment following a protocol previously described in detail (Mauro et al., 2025; Vicente, Villanueva, et al., 2025). Briefly, distilled water was added to the native starches, considering their initial moisture content, to adjust the final moisture content to 25%. Samples were incubated at 4 °C overnight for moisture equilibrium, after which they were stored at −20 °C in sealed bags. Prior to microwave treatment, the samples were brought to 25 °C, and 120 g of each starch was placed in heat-resistant, hermetic, glass containers.

Microwave treatments were conducted using a customised microwave oven (Sharp R-342(IN)W, Osaka, Japan), operating at 900 W and 2450 MHz, with a computer-controlled system to regulate the microwave application pattern and time. Sample temperature was increased from 25 to 100 °C within 5 min and subsequently maintained at 100 ± 3 °C for 25 min through computer-controlled on/off modulation of the magnetron. The magnetron was only active for ~3.6 min during the whole 30-min period. Treatment conditions were established based on preliminary testing to obtain desirable molecular and functional modification. After treatment, the starches were dried at 35 °C until reaching a moisture content similar to that of the original samples (~12%). They were then disaggregated using a mortar and ground in a 150 W Moulinex A505 blade mill. Finally, the samples were sieved through a 250 μm mesh (ASTM). Subsequently, the samples were stored in hermetically sealed bags at 4 °C until analysis.

2.3. High-performance anion exchange chromatography with pulsed amperometric detection (HPAEC/PAD)

Approximately 2 mg of sample was suspended in 1 mL of 50 mM sodium acetate buffer (pH 4.0), incubated at 99 ± 1 °C for 60 min in a ThermoMixer® (Eppendorf, Germany), and cooled to 40 °C. Subsequently, 4 μL of isoamylase (E-ISAMY, Neogen Megazyme, MI, USA) was added and incubated at 40 ± 1 °C for 3 h and at 99 ± 1 °C for 10 min. Samples were cooled to room temperature and filtered through 0.45 μm prior to injection. Chromatographic separation was performed using a HPAEC/PAD system (Dionex, Sunnyvale, CA, USA), equipped with a Dionex Carbopac PA-200 column and using the Chromeleon 6.80 software. The chromatographic elution followed the established protocol as described (Tian et al., 2023; Wang et al., 2024). Briefly, the elution started with 15% water and 85% 1 M sodium acetate containing 25 mM NaOH. During the run, the proportion of 1M NaOH was increased linearly from 0% to 70%, while sodium acetate decreased to 15%. Amylopectin chain fractions were grouped into A chains (DP 6 to 12), B1 chains (DP 13 to 24), B2 chains (DP 25 to 36) and B3 chains (DP ≥ 37) based on the profile of chain proportions of each degree of polymerisation (DP) of glucose chains (Huang et al., 2024; C. Li, Li, et al., 2020).

2.4. Size-exclusion chromatography coupled with multi-angle light scattering, refractive index, and viscometric multi-detection (SEC/MALS-dRI-visco)

For the evaluation of amylose and amylopectin chains, starch samples were enzymatically debranched using a well-established and widely applied procedure, with minor operational modifications as described in Vela et al. (2023). Briefly, starch was dissolved in DMSO containing 0.5% LiBr (w/w) at 80 °C overnight to ensure complete solubilisation, precipitated twice with ethanol, re-suspended in hot Milli-Q water, debranched with iso-amylase (Megazyme International, Wicklow, Ireland) for 3 h at 37 °C, and freeze-dried. Before analysis, samples were reconstituted in the mobile phase to a final concentration of 4 mg/mL.

The SEC system used was an Agilent 1260 (Agilent Technologies,

Santa Clara, CA, USA) equipped with an online multi-angle light scattering (MALS) (Dawn WD3–04, Wyatt Technology), an Optilab differential refractive index (dRI) detector (Optilab WOP1–03, Wyatt Technology) and a Viscostar viscometer (Wyatt Technology, Santa Barbara, CA, USA). The stationary phase consisted of a GRAM pre-column, GRAM 100 and GRAM 1000 analytical columns (PSS GmbH, Mainz, Germany) connected in series. The mobile phase was DMSO/LiBr (0.5% w/w) at 80 °C and 0.5 mL/min. Pullulan standards (PSS PUL-KIT, 300–700,000 Da; and PSS-PUL1.3M, 1,300,000 Da) were used to calibrate the relation of molecular mass to hydrodynamic radius. Mass percentages were expressed as a function of the degree of polymerisation (DP). The amylopectin regions, AP1 (short chains) and AP2 (long chains), corresponded to the double-peak zone up to approximately DP 100. Amylose fractions were defined as AM1 (DP ~100–300), AM2 (DP 300–1600), and AM3 (DP > 1600). Percentages were obtained by integrating dRI chromatograms. Total amylopectin (APT = AP1 + AP2) and total amylose (AMT = AM1 + AM2 + AM3) were calculated.

For the analysis of whole amylopectin molecules, the same protocol was followed without enzymatic debranched, with a final sample concentration of 1 mg/mL. SEC was performed on the same system using a pre-column and GRAM 100 and GRAM 3000 columns (PSS GmbH, Mainz, Germany) in series, and a flow rate of 0.2 mL/min. Data were processed using ASTRA 8.1.2 software (Wyatt Technology, Waters Corporation, Santa Barbara, USA). The number- and weight-average molecular masses (M_n, M_w), and molecular dispersion or polydispersity index (Đ) were calculated according to Mauro et al. (2025). Radius-related parameters were determined based on the understanding that the radius of gyration (R_g) represents the average spatial size and mass distribution of a macromolecule, whereas the hydrodynamic radius (R_h) corresponds to its effective size related to mobility and diffusion in solution (Haydukivska et al., 2020). Intrinsic viscosity ([η]) was determined according to Dobrynin et al. (2023), providing insight into the contribution of amylopectin to solution viscosity. Radii and intrinsic viscosity values were expressed as z-averages (r_gz, r_gh and [η]) to maintain comparability with published data (Vicente, Mauro, et al., 2025).

2.5. Rapid visco analyser (RVA)

Pasting tests were performed using a rapid visco analyser (RVA-4500, Perten, PerkinElmer Inc., Waltham, MA, USA), applying the time–temperature–shear profile of the STD1 test described in AACC Method 76–21.02 (Cereals & Grains Association, 2010). The pastes were prepared with a concentration of 10 g starch (dry basis)/100 g dispersion. The pasting profiles were analysed using TCW3 Termocline for Windows 3.0 software (Perten Instruments, Australia), from which the parameters peak viscosity (PV), trough viscosity (TV), breakdown viscosity (BV), final viscosity (FV), setback viscosity (SV), pasting temperature (PT) and peak time (Ptime) were extracted in accordance with methodology previously described (C. Li, Li, et al., 2020; Mauro et al., 2023).

2.6. Oscillatory rheology

Dynamic oscillatory analysis was conducted to evaluate the viscoelastic behaviour of starch gels prepared as described in Section 2.5, using a Kinexus Pro + rheometer (Malvern Instruments Ltd., Malvern, UK). The measurements were performed with 40 mm serrated parallel plates, set at a 1 mm gap and 25 °C. Prior to testing, the samples were placed between the plates and allowed to rest for 5 min to relax stresses and standardize the time for gel structuring. To prevent water evaporation during measurements, a solvent trap was used and a thin layer of Vaseline oil was applied around the edge of the measuring geometry. Strain sweeps were performed at 1 Hz over a strain range of 0.1–1000%, extended to 2500% for potato and tapioca gels. From these tests, the linear viscoelastic region (LVR), the maximum stress and strain within the LVR (MaxStress and MaxStrain, respectively), and the stress and strain at the crossover point where $G' = G''$ (CPstress and CPstrain, respectively) were determined. Frequency sweeps were conducted within the LVR at a fixed strain of 1%, over a frequency range of 10–1 Hz. The resulting data were fitted to the power-law model described by Ronda et al. (2013). The parameters G_1', G_1'', and $(\tan\delta)_1$ represent the fitted values of the elastic modulus, viscous modulus, and loss tangent, respectively, at 1 Hz. The exponents *a*, *b*, and *c* describe the frequency dependence of dynamic moduli and loss tangent.

2.7. Statistical analysis

Mean values and standard deviations were calculated, and differences among treatments were evaluated by one-way analysis of variance (ANOVA) followed by Tukey's multiple comparison test, using Statgraphics Centurion 19 v.19.4.01 (Statgraphics Technologies Inc., The Plains, VA, USA). Pearson correlation matrices and principal component analysis (PCA) were performed with OriginPro 2024b (OriginLab Corporation, Northampton, MA, USA).

3. Results and discussion

3.1. Amylopectin chain-length distribution obtained from HPAEC/PAD

The distribution of amylopectin chains by DP, along with the differences in this distribution between untreated and microwave-treated samples, is illustrated in Fig. 1, while the relative proportions of chain types (A, B1, B2, and B3) are summarised in Table 1.

Among the untreated starches, wheat, tapioca, and potato exhibited the highest proportions of A and B1 chains and the lowest of B2 and B3 chains, consistent with previous reports (Yang et al., 2021; Zhao et al., 2023; Zheng et al., 2023). In contrast, starches from rice and maize, both normal and waxy, showed the opposite trend, with lower proportions of A and B1 chains and higher proportions of B2 and B3 chains.

Microwave treatment markedly induced source-dependent changes in the amylopectin chain-length distribution. The most pronounced increases in A-chains were observed in waxy starches, with a rise in the proportion of A-chains after treatment of +3.1% in waxy rice and +2.3% in waxy maize. B1-chains also increased markedly in these waxy samples (+4.7 and +4.4%, respectively). This shift towards shorter chains is consistent with the partial hydrolytic effect of microwave treatment (Mauro et al., 2025), which promotes cleavage of amylopectin branches.

Changes in B2-chains varied across starch types. There was a decrease in waxy samples, while tapioca and non-waxy cereals showed increases, the most pronounced in wheat (from 19.6% to 22.1%). B3 chains declined notably in waxy cereals (~35% relative reduction), followed by normal rice and normal maize starches, confirming a general loss of the longest amylopectin branches after treatment.

The tapioca and wheat starches exhibited counter-intuitive behaviours, characterised by decreases in short amylopectin chains (A) and increases in longer chains (B2 and B3). Specifically, the A-chain contents decreased 1.9% in tapioca and 1.1% in wheat. Tapioca also showed a marked increase in B2 and B3-chains, with B3 reaching nearly 21% (Fig. 1G). The wheat starch displayed a similar pattern, with a notable increase in B2 chains and only a minor decrease in B3 chains (Fig. 1E). This behaviour may stem from fragmentation of very long amylose molecules producing chains with DP values similar to long amylopectin chains (see Section 3.2).

Finally, potato starch exhibited minimal changes after microwave treatment, with only slight, non-significant variations in B1 and B2 chains. This limited response may be linked to its distinctive granular structure or high degree of phosphorylation, potentially reducing susceptibility to microwave-induced hydrolysis (Zhou et al., 2024).

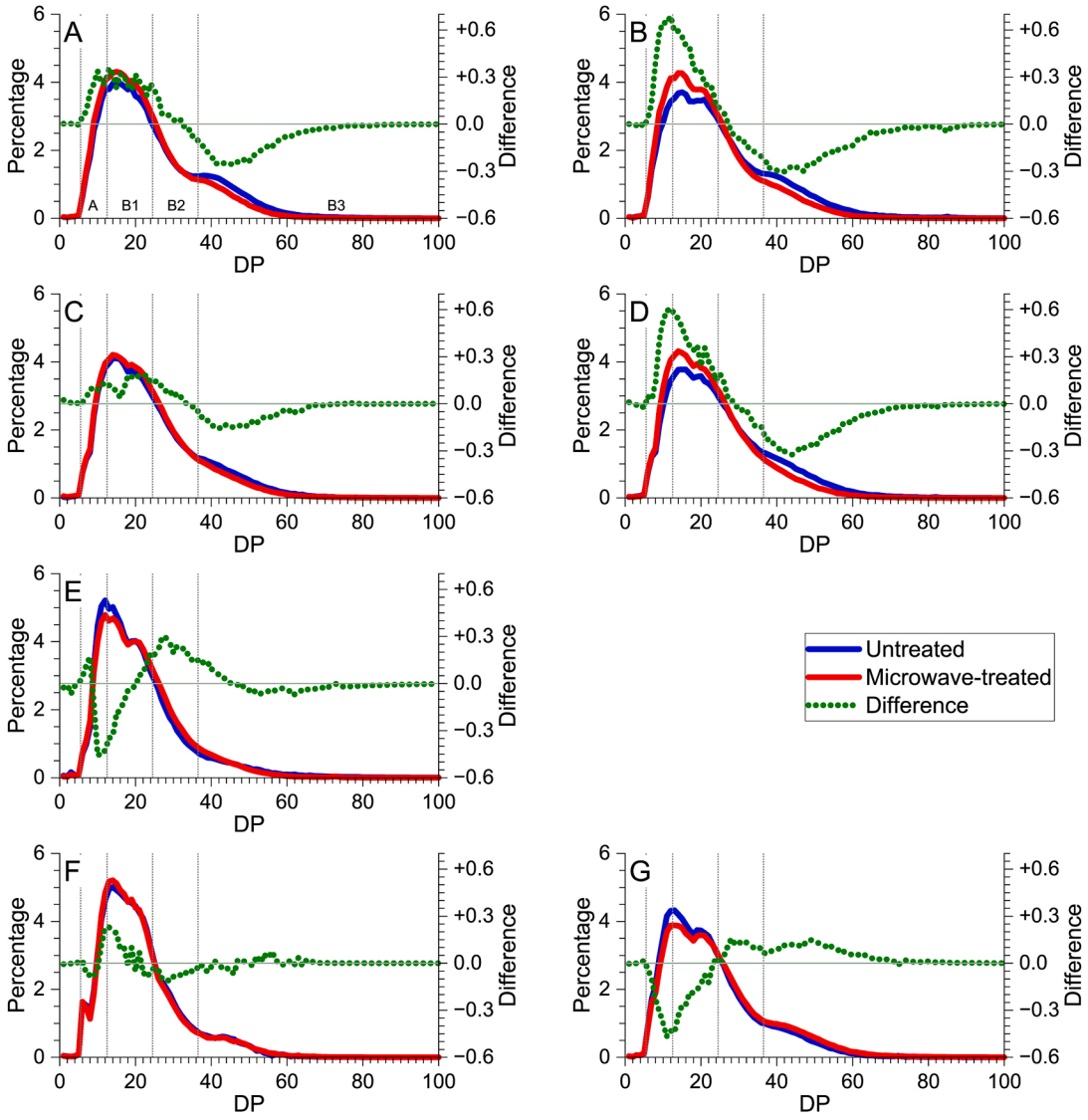

Fig. 1. Amylopectin chain-length distribution (percentage vs. degree of polymerisation, DP; left y-axis) and treatment-induced percentage differences (treated – untreated; right y-axis), determined by HPAEC/PAD. (A) normal rice, (B) waxy rice, (C) normal maize, (D) waxy maize, (E) wheat, (F) potato, (G) tapioca. Vertical dotted lines indicate the DP ranges defining each chain type: A (DP 6–12), B1 (DP 13–24), B2 (DP 25–36), and B3 (DP ≥ 37).

Table 1
Percentages of amylopectin chain fractions in starches determined by HPAEC/PAD.

		A	B1	B2	B3
Normal Rice	U	16.6 ± 0.1^{f}	44.0 ± 0.2^{fg}	20.9 ± 0.1^{ef}	18.5 ± 0.3^{ab}
	T	18.1 ± 0.8^{cd}	47.2 ± 1.0^{c}	21.3 ± 0.5^{e}	13.4 ± 1.2^{e}
Waxy Rice	U	16.1 ± 0.1^{f}	41.4 ± 0.2^{h}	22.9 ± 0.1^{bcd}	19.6 ± 0.3^{a}
	T	19.2 ± 0.2^{bc}	46.1 ± 0.4^{cde}	21.9 ± 0.1^{cde}	12.8 ± 0.3^{e}
Normal Maize	U	16.1 ± 0.1^{f}	44.8 ± 0.1^{ef}	23.2 ± 0.1^{abc}	15.9 ± 0.3^{cd}
	T	16.7 ± 0.7^{ef}	46.5 ± 0.8^{cd}	23.8 ± 0.1^{ab}	13.0 ± 1.5^{e}
Waxy Maize	U	14.8 ± 0.1^{g}	42.5 ± 0.2^{gh}	24.5 ± 0.1^{a}	18.2 ± 0.3^{abc}
	T	17.1 ± 0.1^{def}	46.9 ± 0.8^{c}	24.3 ± 0.4^{ab}	11.7 ± 0.5^{ef}
Wheat	U	21.2 ± 0.2^{a}	49.8 ± 0.8^{b}	19.6 ± 0.6^{fg}	9.4 ± 1.6^{fg}
	T	20.1 ± 0.2^{b}	49.0 ± 0.1^{b}	22.1 ± 0.2^{cde}	8.8 ± 0.1^{g}
Potato	U	18.2 ± 0.1^{cd}	53.4 ± 0.1^{a}	19.3 ± 0.1^{g}	9.1 ± 0.1^{g}
	T	18.1 ± 0.1^{cd}	54.0 ± 0.2^{a}	18.8 ± 0.1^{g}	9.1 ± 0.2^{g}
Tapioca	U	19.7 ± 0.2^{b}	45.1 ± 0.8^{def}	21.7 ± 0.7^{de}	13.5 ± 1.7^{de}
	T	17.8 ± 0.8^{de}	43.0 ± 0.6^{gh}	22.8 ± 1.4^{bcd}	16.4 ± 0.1^{bc}

Results are expressed as %, mean ± standard deviation. U = untreated starches, T = microwave-treated starches. Different letters indicate significantly different means (Tukey test, α = 0.05). Chain types according to degree of polymerisation: A (DP 6–12), B1 (DP 13–24), B2 (DP 25–36), and B3 (DP ≥ 37).

3.2. Amylose and amylopectin chain-length distribution obtained from SEC/MALS-dRI-Visco

The chain-length distribution of amylose and amylopectin branched chains, as determined by size-exclusion chromatography (SEC) combined with MALS-dRI-Visco multi-detection, are presented in Fig. 2 and the grouped proportions of chain types are summarised in Table 2.

The amylose content of starches, obtained from the relative area in dRI profile, varied in the order: wheat (37.2%) = normal maize (35.6%) > tapioca (26.6%) = normal rice (25.6%) > potato (22.6%) > waxy rice and maize (<3.5%). Among the amylose fractions, AM3, representing the longest chains, was most abundant in wheat (22.4%) and tapioca (21.4%). Potato starch also showed a significantly high AM3 proportion (16.6%). As expected, waxy starches exhibited very low AM3 content (<1.2%), consistent with their minimal amylose levels. The intermediate fraction (AM2) was particularly high in normal maize (19.0%) and wheat (12.7%), while the shortest amylose chains (AM1) were generally present in low amounts, with the highest level observed in normal maize (5.1%).

The amylose peak DP value (AMpeak), corresponding to the degree of polymerisation with the highest concentration within the amylose

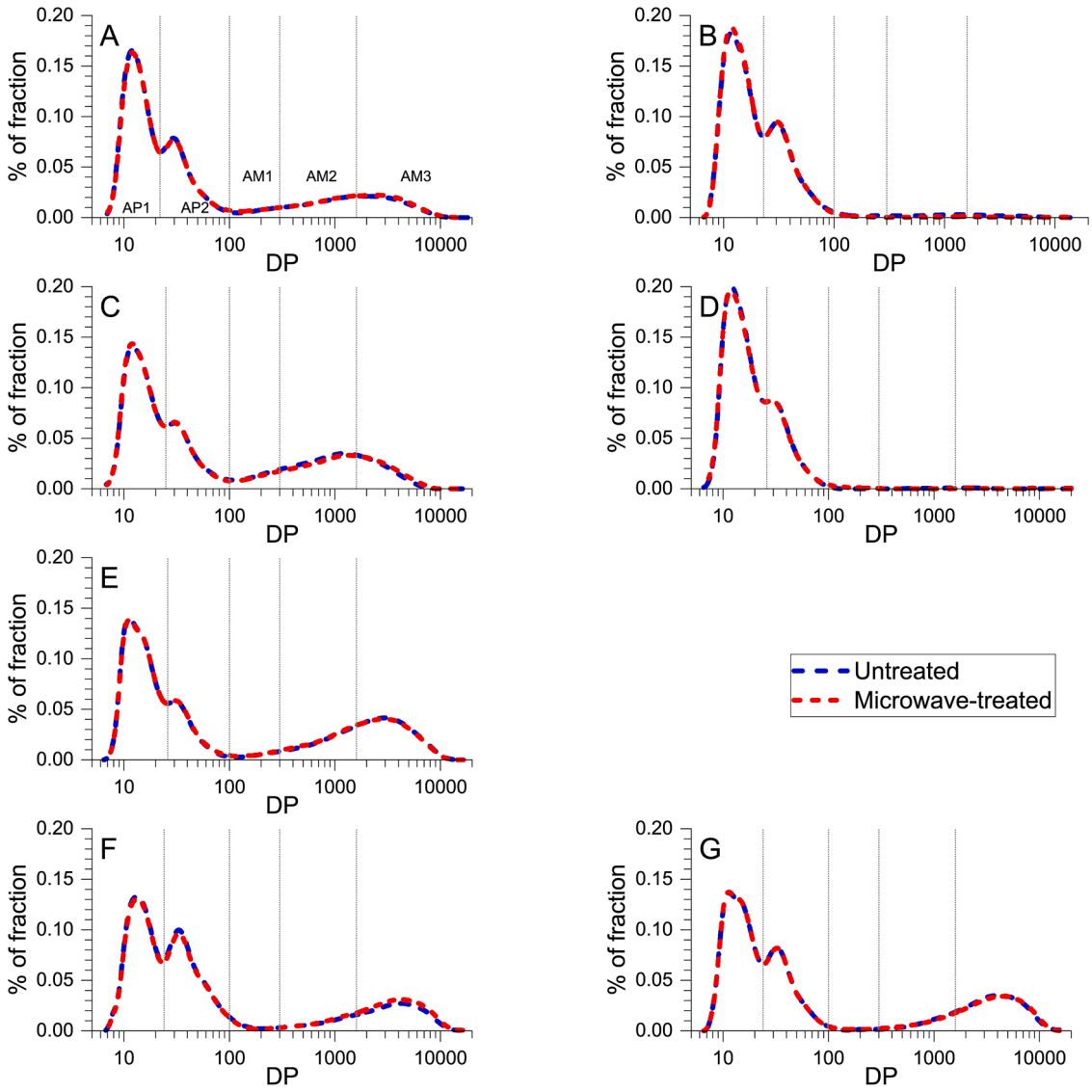

Fig. 2. Chain-length distribution of amylose and debranched amylopectin as a function of the degree of polymerisation (DP) obtained by SEC/MALS-dRI-Visco. (A) normal rice, (B) waxy rice, (C) normal maize, (D) waxy maize, (E) wheat, (F) potato, (G) tapioca.

Table 2
Chain-length distribution of amylose and debranched amylopectin chains determined by SEC/MALS-dRI-Visco.

		AM1 (%)	AM2 (%)	AM3 (%)	AMT (%)	AMpeak (DP)	AP1 (%)	AP2 (%)	APT (%)
Normal Rice	U	2.6 ± 0.3^{bc}	11.0 ± 0.3^{d}	11.9 ± 0.9^{b}	25.6 ± 0.9^{c}	2023 ± 265^{bc}	50.0 ± 0.2^{e}	24.4 ± 1.1^{c}	74.4 ± 0.9^{b}
	T	2.8 ± 0.1^{c}	11.0 ± 0.1^{d}	12.3 ± 0.1^{b}	26.1 ± 0.1^{c}	2301 ± 291^{c}	49.2 ± 0.1^{e}	24.7 ± 0.1^{cd}	73.9 ± 0.1^{b}
Waxy Rice	U	0.5 ± 0.3^{a}	1.7 ± 0.7^{b}	1.2 ± 0.8^{a}	3.4 ± 1.6^{a}	1648 ± 169^{abc}	64.4 ± 0.9^{f}	32.2 ± 0.7^{e}	96.6 ± 1.6^{d}
	T	0.4 ± 0.3^{a}	0.3 ± 0.2^{a}	0.0 ± 0.1^{a}	0.6 ± 0.4^{a}	1540 ± 117^{ab}	66.5 ± 0.3^{g}	32.8 ± 0.2^{e}	99.4 ± 0.4^{d}
Normal Maize	U	5.1 ± 0.1^{d}	19.0 ± 0.1^{f}	11.5 ± 0.6^{b}	35.6 ± 0.5^{d}	1273 ± 49^{a}	44.8 ± 0.1^{b}	19.6 ± 0.5^{b}	64.4 ± 0.5^{a}
	T	4.9 ± 0.3^{d}	17.7 ± 0.2^{f}	12.9 ± 0.7^{b}	35.4 ± 0.6^{d}	1365 ± 3^{a}	45.0 ± 0.7^{bc}	19.6 ± 0.2^{b}	64.6 ± 0.6^{a}
Waxy Maize	U	0.2 ± 0.2^{a}	0.4 ± 0.7^{ab}	0.6 ± 0.5^{a}	1.2 ± 0.9^{a}	1160 ± 41^{a}	72.5 ± 0.7^{h}	26.3 ± 0.3^{cd}	98.8 ± 0.9^{d}
	T	0.1 ± 0.2^{a}	0.5 ± 0.3^{ab}	0.2 ± 0.2^{a}	0.8 ± 0.4^{a}	1120 ± 60^{a}	72.6 ± 0.4^{h}	26.6 ± 0.1^{d}	99.2 ± 0.4^{d}
Wheat	U	2.1 ± 0.3^{b}	12.7 ± 0.1^{e}	22.4 ± 0.9^{d}	37.2 ± 0.6^{d}	2982 ± 91^{d}	46.7 ± 0.3^{cd}	16.1 ± 0.8^{a}	62.8 ± 0.6^{a}
	T	2.1 ± 0.1^{b}	12.8 ± 0.6^{e}	22.9 ± 0.8^{d}	37.9 ± 0.3^{d}	3044 ± 178^{d}	46.0 ± 0.3^{bcd}	16.1 ± 0.1^{a}	62.1 ± 0.3^{a}
Potato	U	0.4 ± 0.1^{a}	5.6 ± 0.3^{c}	16.6 ± 0.9^{c}	22.6 ± 1.3^{b}	4117 ± 47^{e}	41.1 ± 0.8^{a}	36.3 ± 0.6^{f}	77.4 ± 1.3^{c}
	T	0.5 ± 0.2^{a}	5.9 ± 0.1^{c}	18.2 ± 0.8^{c}	24.6 ± 0.7^{bc}	4152 ± 115^{e}	40.1 ± 0.1^{a}	35.3 ± 0.8^{cf}	75.4 ± 0.7^{bc}
Tapioca	U	0.3 ± 0.2^{a}	4.8 ± 0.3^{c}	21.4 ± 0.1^{d}	26.6 ± 0.1^{c}	4393 ± 343^{e}	47.2 ± 0.5^{d}	26.2 ± 0.6^{cd}	73.4 ± 0.1^{b}
	T	0.4 ± 0.1^{a}	5.0 ± 0.4^{c}	21.5 ± 0.2^{d}	27.0 ± 0.2^{c}	4539 ± 52^{e}	47.1 ± 0.1^{d}	25.9 ± 0.2^{cd}	73.0 ± 0.2^{b}

Values are expressed as mean ± standard deviation. Different letters indicate significantly different means (Tukey's test, α = 0.05). U = untreated starch, T = microwave-treated starch, AM1 = amylose short chains, AM2 = amylose medium chains, AM3 = amylose long chains, AMT = total amylose, AMpeak = degree of polymerisation at maximum concentration, AP1 = amylopectin short chains, AP2 = amylopectin long chains, APT = total amylopectin.

region, was highest in tapioca (DP 4393), followed by potato (DP 4117) and wheat (DP 2982). In general, higher AM peak values were

associated with a greater AM3 content. The elevated AM3 and AMpeak values in wheat and tapioca reinforce the hypothesis that very long amylose chains in these samples are more prone to microwave-induced fragmentation, producing fragments with DP values comparable to those of long amylopectin chains. This may account for the observed relative decrease in A and B1 chains following microwave treatment in these two starches (Table 1), accompanied by a relative increase in some specific B3 chains. The SEC/MALS-dRI-Visco data support the interpretation based on the chain-type distribution derived from HPAEC/PAD, where it was postulated that some of the long amylose fragments may have been detected as amylopectin chains.

All starches showed a predominance of short-chain amylopectin (AP1) over long-chain amylopectin (AP2), as illustrated in Fig. 2 and detailed in Table 3. This is consistent with the higher abundance of A + B1 chains compared to B2 + B3 chains observed in the HPAEC/PAD data. However, direct comparisons between individual AP1 and AP2 fractions across samples do not always mirror the trends observed in HPAEC/PAD-derived groupings. Thus, the chain grouping profiles obtained by SEC/MALS-dRI-Visco may differ slightly from those determined by HPAEC/PAD. The amylopectin distribution displayed a clear bimodal pattern in all samples, with a cut-off region between DP 22 and DP 26 (Fig. 2).

Potato starch exhibited the highest proportion of AP2 chains (36.3%). This result differs from the HPAEC/PAD data, in which both potato and wheat starches were characterised by a higher abundance of shorter chains. This apparent divergence may be attributed to the relatively narrow peak obtained from SEC/MALS-dRI-Visco centred around DP 35, the presence of longer B1 chains and shorter B2 chains, as well as potential overlap of signals from chains with very similar DP. The simultaneous presence of both short and long amylopectin chains in potato starch has been previously reported (Genkina et al., 2007), and is considered a key factor underlying its distinctive viscoelastic behaviour, as discussed in later sections.

In contrast, wheat (16.1%) and normal maize (19.6%) exhibited the lowest AP2 proportions. Notably, wheat starch was the only in which the AM3 fraction (22.4%) exceeded the AP2 proportion, reflecting an unusually high content of long amylose chains. The elevated AP1 content in wheat also corresponded well with its high A-chain proportion, as reported in Table 1.

Interestingly, SEC/MALS-dRI-Visco analysis revealed no significant differences in the overall chain-length distribution after microwave treatment, indicating that the global distribution of long linear chains, particularly those associated with amylose, remained largely unchanged under the conditions applied (Table 2, Fig. 2). This contrasts with the findings based on HPAEC/PAD (Table 1 and Fig. 1), where meaningful shifts in chain-type proportions were observed with microwave treatment. A potential explanation lies in the inherent limitations of SEC/MALS-dRI-Visco in detecting subtle molecular-level structural changes, particularly for long linear chains such as amylose. The resolution of SEC can be compromised by band broadening effects, particularly when analysing components with a wide DP range (C. Li, Li, et al., 2020). Furthermore, α(1 → 6) linkages, which define the branching points in amylopectin, are generally more susceptible to microwave-induced cleavage than the α(1 → 4) linkages that dominate linear segments (Tian et al., 2023). Consequently, molecular modifications are expected to be more pronounced in amylopectin fine structure than in amylose, and changes affecting already short chains or low-molecular-weight fractions may not be readily detected by SEC, as observed in the present study using SEC/MALS-dRI-Visco on debranched samples.

Importantly, the absence of major changes in amylose chain-length distributions suggests that the contribution of amylose to the observed viscoelastic modifications is more closely related to structural reorganisation and redistribution at the supramolecular level rather than to detectable molecular-level degradation. Nevertheless, minor alterations in chain architecture can exert significant influence on starch functionality (Bertoft et al., 2016), as will be discussed in the following sections.

3.3. Molecular properties of whole amylopectin obtained from SEC/MALS-dRI-Visco

The molecular size characteristics of whole amylopectin molecules are summarised in Table 3, while the concentration distribution profiles of molecular weight, radius of gyration (R_g), and hydrodynamic radius (R_h) are depicted in Fig. 3.

Size-exclusion chromatography of very large and flexible macromolecules, such as whole starch molecules, is known to be affected by shear-induced degradation during separation (Cave et al., 2009). Accordingly, SEC-derived molecular weight distributions were interpreted in a comparative manner, focusing on relative trends rather than absolute molecular weight values. Despite these inherent limitations, the trends observed for whole starch molecules were consistent with those previously obtained for the same untreated and microwave-treated samples analysed by asymmetric flow field-flow fractionation (AF4) (Mauro et al., 2025), supporting the validity of the comparative interpretations presented.

Among the untreated samples, potato starch exhibited the lowest molecular weights, followed by waxy rice starch. In contrast, waxy maize and wheat starches displayed the highest molecular weights, in agreement with previous results obtained using Asymmetric Flow Field-Flow Fractionation (AF4) on the same materials (Mauro et al., 2025).

Table 3
Molecular parameters of whole amylopectin molecules obtained by SEC/MALS-dRI-Visco.

Starch		M_n	M_w	Đ	R_gz	R_hz	R_gz/R_hz	[η]z
Normal Rice	U	136± 6^{d}	288 ± 14^{ef}	2.13 ± 0.01^{j}	223 ± 11^{defg}	242 ± 12^{ef}	0.92 ± 0.01^{d}	239 ± 10^{cd}
	T	138± 6de	260 ± 12^{d}	1.88 ± 0.01^{i}	199 ± 10^{bc}	232 ± 11^{def}	0.86 ± 0.01^{bc}	242 ± 10^{cde}
Waxy Rice	U	122± 5^{cd}	192± 8^{b}	1.58 ± 0.01^{f}	210 ± 10^{cde}	196± 8^{bc}	1.06 ± 0.01^{i}	206± 9^{b}
	T	70± 3^{a}	102± 5^{a}	1.46 ± 0.01^{d}	186± 8^{b}	150± 7^{a}	1.25 ± 0.01^{j}	157± 7^{a}
Normal Maize	U	166± 7^{f}	270 ± 13de	1.62 ± 0.01^{g}	218 ± 10^{cdef}	236 ± 11^{ef}	0.93 ± 0.01^{d}	243 ± 11^{cde}
	T	130± 6^{d}	230 ± 10^{c}	1.77 ± 0.01^{h}	212± 9^{cde}	220± 9^{cde}	0.96 ± 0.01^{e}	226 ± 10^{bcd}
Waxy Maize	U	233 ± 11^{g}	367 ± 16^{h}	1.58 ± 0.01^{f}	245 ± 10^{g}	252 ± 11^{f}	0.97 ± 0.01^{f}	233 ± 11^{bcd}
	T	160± 7^{f}	285 ± 13^{def}	1.78 ± 0.01^{h}	238 ± 10^{fg}	233 ± 10^{def}	1.02 ± 0.01^{h}	214± 9^{bc}
Wheat	U	319 ± 15^{i}	328 ± 16^{g}	1.03 ± 0.01^{a}	207± 9^{bcde}	243 ± 10^{ef}	0.85 ± 0.01^{b}	273 ± 12^{e}
	T	281 ± 13^{h}	309 ± 13^{fg}	1.10 ± 0.01^{b}	202± 9^{bcd}	234 ± 10^{ef}	0.86 ± 0.01^{bc}	252 ± 12de
Potato	U	105± 5^{bc}	120± 6^{a}	1.14 ± 0.01^{c}	159± 8^{a}	184± 9^{b}	0.86 ± 0.01^{c}	320 ± 13^{f}
	T	96± 4^{b}	110± 5^{a}	1.15 ± 0.01^{c}	156± 7^{a}	209 ± 10^{cd}	0.75 ± 0.01^{a}	496 ± 23^{g}
Tapioca	U	157± 7^{ef}	229 ± 11^{c}	1.46 ± 0.01^{d}	230 ± 10^{efg}	233 ± 10^{def}	0.99 ± 0.01^{g}	311 ± 14^{f}
	T	119± 6^{cd}	176± 8^{b}	1.48 ± 0.01^{e}	217± 9^{cdef}	220 ± 10^{cde}	0.98 ± 0.01^{g}	332 ± 15^{f}

Values are expressed as mean ± standard deviation. Different letters indicate significantly different means (Tukey's test, α = 0.05). U = untreated starch, T = microwave-treated starch, M_n = number-based molecular mass (× 10^6 Da), M_w = weight-based molecular mass (× 10^6 Da), Đ = molecular mass dispersity (M_w/M_n), R_gz = z-average radius of gyration (nm), R_hz = z-average hydrodynamic radius (nm), [η]z = z-average intrinsic viscosity (mL/g).

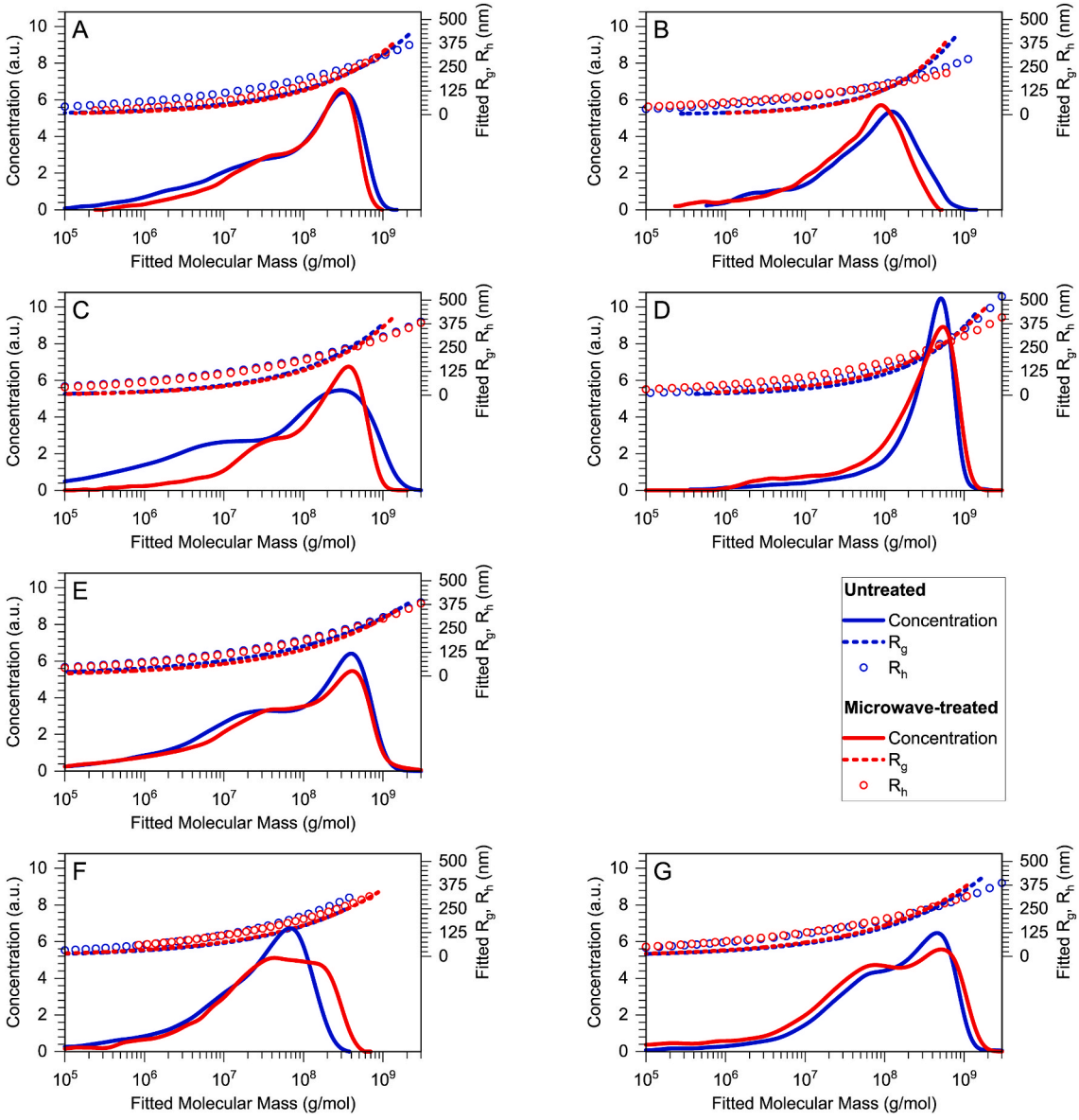

Fig. 3. SEC/MALS-dRI-Visco profiles of whole starch molecules showing concentration (arbitrary units, left y-axis), radius of gyration (R_g) and hydrodynamic radius (R_h) (right y-axis) as a function of fitted molecular mass. (A) normal rice, (B) waxy rice, (C) normal maize, (D) waxy maize, (E) wheat, (F) potato, (G) tapioca.

Notable differences in number-average (M_n) and weight-average (M_w) molecular weights were observed between the waxy and non-waxy varieties of rice and maize, the non-waxy ones showing higher molecular mass dispersity (Đ) than the waxy ones (Table 3). In contrast, potato and tapioca starches exhibited lower Đ values, alongside native wheat starch, the only cereal sample with a Đ value close to 1.

Molecular size was evaluated by the z-average radius of gyration (R_gz) and hydrodynamic radius (R_hz), as explained in section 2.4. These two parameters offer complementary insights: while R_gz reflects the average distance of polymer segments from the centre of mass and indicates the overall spatial distribution of the molecule; R_hz is associated with the diffusion of the polymer in solution, determined by its interaction with the surrounding solvent (Nygaard et al., 2017). The R_gz/R_hz ratios ranged from 0.8 to 1.3. This is consistent with a compact, highly branched amylopectin conformation in solution, in which the high density of α(1 → 6) branching limits chain extension and favours globular-like arrangements under conditions of complete starch solubilisation, as reported by Guo et al. (2019).

Regarding the absolute size values, potato starch showed the smallest dimensions across all samples, with 159 nm in R_gz and 184 nm in R_hz. Wheat starch also exhibited relatively small radii (R_gz of 207 nm and R_hz of 243 nm), which, when considered alongside its high molecular weight (Mn of 319 × 10^6 Da and Mw of 328 × 10^6 Da), is indicative of a more compact molecular conformation, an observation that is consistent with previous findings on wheat starches (Mauro et al., 2025).

Intrinsic viscosity values ([η]) are also reported in Table 3. For rigid macromolecules, [η] correlates with molecular shape, whereas for flexible polymers, it is influenced by intramolecular interactions and solvent–solute interactions (Hernández-Cifre et al., 2025). Among the untreated samples, potato and tapioca exhibited the highest [η] values, followed by the non-waxy cereals, and finally the waxy cereal starches. No clear correlation was observed between intrinsic viscosity and molecular weight. In potato and to a lesser extent in tapioca, phosphorylation may increase starch viscosity by enhancing hydration and limiting interchain association, thereby increasing the effective molecular surface of amylopectin available for intermolecular interactions (Blennow et al., 2001; Kasemsuwan & Jane, 1996).

Following microwave treatment, the most pronounced reductions in

M_n and M_w were observed in waxy rice starch, followed by the waxy maize starch. The inherently low amylose content in these starches likely rendered them more susceptible to microwave-induced hydrolysis (Mauro et al., 2025). All samples exhibited some degree of molecular mass reduction, consistent with the hydrolytic nature of the treatment. Importantly, this reduction reflects partial fragmentation of the whole starch molecules rather than uniform shortening of individual chains, and its magnitude varied across samples. Notably, potato starch exhibited the smallest decrease in molecular weight, consistent with its relatively unaltered structure observed in the HPAEC/PAD analyses.

Molecular radii also tended to decrease after treatment, with one exception: the hydrodynamic radius of treated potato starch increased significantly. This may be attributed to the unfolding of molecular chains and an increase in apparent size due to aggregation (Xu et al., 2021).

In terms of intrinsic viscosity changes, most starches retained values similar to their native counterparts. Two notable exceptions were observed. Waxy rice starch exhibited a marked reduction in [η], which can be attributed to extensive hydrolysis during treatment. In contrast, potato starch showed a substantial increase in [η], likely related to structural unfolding and expansion following treatment (Xu et al., 2021).

3.4. Pasting properties

Pasting profiles are illustrated in Fig. 4, and the derived pasting parameters are summarised in Table 4.

Among the untreated samples, potato starch exhibited the highest peak viscosity (PV), exceeding 12,000 mPa s, more than twice that of the other starches. This was followed by tapioca starch, with a PV above 6000 mPa s. The waxy cereal starches displayed intermediate values, while non-waxy cereal starches exhibited the lowest PV values (3200–4000 mPa s). This behaviour could be attributed to the higher amylopectin content of potato, tapioca, and the waxy cereal starches, which contributes to greater granule integrity and swelling capacity (Mauro et al., 2023). Potato and tapioca starches also showed the lowest AP1/AP2 ratios, indicating a greater proportion of long amylopectin chains, which is typically associated with enhanced granule stability and higher PV values (Chen & Zhu, 2024). However, the most important factor is likely the high starch-phosphate ester content in the potato, and medium phosphate content in tapioca starches (Blennow & Engelsen, 2010; Ding et al., 2024; Kasemsuwan & Jane, 1996), contributing to

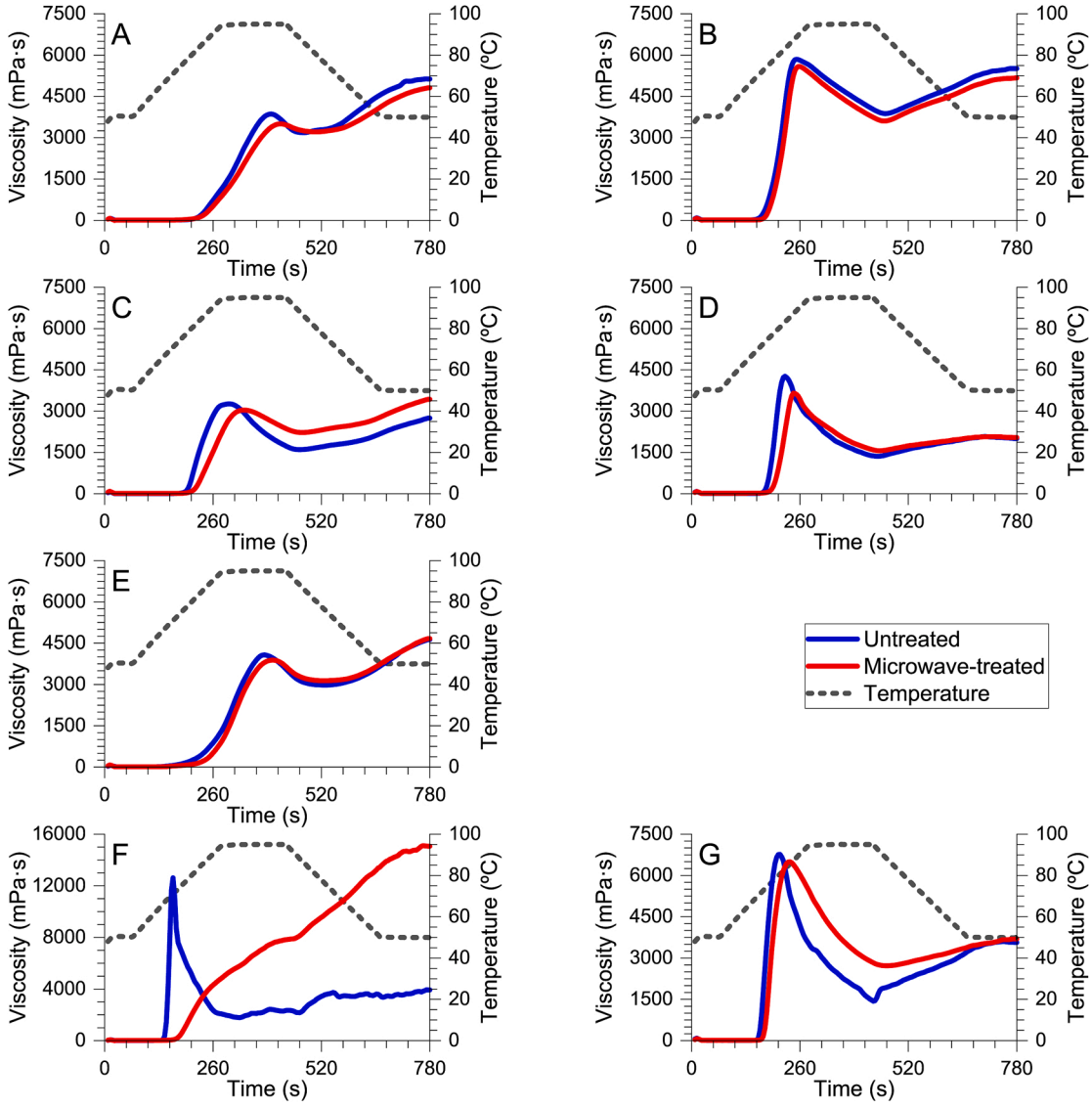

Fig. 4. Pasting profiles of untreated and microwave-treated starches. (A) normal rice, (B) waxy rice, (C) normal maize, (D) waxy maize, (E) wheat, (F) potato, (G) tapioca.

Table 4
Pasting parameters of untreated and microwave-treated starch mixtures (10 g/100 g) obtained by RVA.

Starch		PV	TV	BV	FV	SV	Ptime	PT
Normal Rice	U	3860 ± 44^{cde}	3182 ± 71^{cde}	678 ± 27^{bc}	5132 ± 10de	1950 ± 81^{cd}	6.6 ± 0.1^{h}	82.4 ± 0.1^{f}
	T	3502 ± 35^{abc}	3211 ± 26de	292± 9^{ab}	4814 ± 74^{d}	1603 ± 48^{bcd}	7.0 ± 0.1^{i}	83.7 ± 0.5^{f}
Waxy Rice	U	5850 ± 14^{f}	3876 ± 43^{f}	1975 ± 29^{e}	5514 ± 14^{e}	1639 ± 29^{bcd}	4.2 ± 0.1^{de}	70.2 ± 0.1^{b}
	T	5595 ± 55^{f}	3607 ± 81^{ef}	1988 ± 25^{e}	5171 ± 16de	1564 ± 64^{bcd}	4.3 ± 0.1^{e}	72.1 ± 0.6^{bc}
Normal Maize	U	3266± 9^{ab}	1602 ± 61^{a}	1664 ± 52de	2746 ± 20^{b}	1144 ± 41^{abc}	5.0 ± 0.1^{f}	76.8 ± 0.9^{d}
	T	3064 ± 273^{a}	2223 ± 30^{b}	841 ± 303^{bc}	3431 ± 431^{c}	1208 ± 460^{abc}	5.6 ± 0.3^{g}	79.5 ± 0.6^{e}
Waxy Maize	U	4266 ± 42^{e}	1357 ± 13^{a}	2909 ± 54^{f}	2007 ± 33^{a}	650 ± 45^{a}	3.7 ± 0.1^{bc}	72.7 ± 0.1^{c}
	T	3654 ± 135^{bcd}	1553 ± 33^{a}	2101 ± 147^{e}	2037 ± 86^{a}	484 ± 99^{a}	4.1 ± 0.1^{de}	75.7 ± 0.5^{d}
Wheat	U	4084 ± 71de	2978 ± 169^{cd}	1107 ± 98^{cd}	4633 ± 71^{d}	1655 ± 98^{bcd}	6.4 ± 0.1^{h}	76.6 ± 0.1^{d}
	T	3885± 4^{cde}	3139 ± 30^{cde}	746 ± 34^{bc}	4669 ± 18^{d}	1530 ± 13^{bcd}	6.7 ± 0.1^{hi}	83.6 ± 0.6^{f}
Potato	U	12614 ± 49^{i}	1784 ± 288^{ab}	10831 ± 238^{i}	3936 ± 293^{c}	2153 ± 581^{d}	2.7 ± 0.1^{a}	66.1 ± 0.1^{a}
	T	7879± 8^{h}	7879± 8^{g}	0± 0^{a}	15059 ± 82^{f}	7180 ± 74^{e}	7.5 ± 0.1^{j}	71.4 ± 0.6^{bc}
Tapioca	U	6786± 2^{g}	1417 ± 271^{a}	5369 ± 269^{h}	3565 ± 10^{c}	2149 ± 281^{d}	3.5 ± 0.1^{b}	70.3 ± 0.1^{b}
	T	6504 ± 278^{g}	2722 ± 60^{c}	3782 ± 224^{g}	3697 ± 36^{c}	975 ± 25^{ab}	3.9 ± 0.1^{cd}	72.1 ± 0.4^{bc}

Values are expressed as mean ± standard deviation. Different letters indicate significantly different means (Tukey's test, α = 0.05). U = untreated starch; T = microwave-treated starch; PV = Peak viscosity; TV = Trough viscosity; BV = Breakdown viscosity; FV = Final viscosity; SV = Setback viscosity; Ptime = Peak time (min); PT = Pasting temperature (°C). Viscosities are expressed in mPa·s.

high hydrating and swelling capacity (Viksø-Nielsen et al., 2001) of these starch types.

Untreated waxy and normal rice starches displayed the highest trough viscosities (TV), indicating greater viscosity retention after granule rupture. Wheat followed closely, showing no statistically significant difference from normal rice, since its limited swelling (reflected in its lower PV) was accompanied by a marked resistance to viscosity loss after granule collapse. The remaining starches exhibited statistically similar TV values (~1500 mPa s). The highest breakdown viscosities (BV) were recorded for native potato starch, followed by tapioca, consistent with their high PV and comparatively low TV values. Waxy starches showed intermediate BV values, while non-waxy cereal starches had the lowest, reflecting their low PV and relatively high TV values.

Final viscosities (FV) were highest in waxy and normal rice starches, followed by wheat, samples that already presented the greatest TV values. Tuber starches presented intermediate FV values, while maize starches showed the lowest, consistent with their overall low viscosity profiles. Setback viscosity (SV) was statistically similar across all samples. Tuber starches showed slightly, though non-significantly, higher SV values, followed by normal rice, wheat, and waxy rice starches. Normal and waxy maize starches presented the lowest SV, demonstrating poor viscosity increase during the cooling phase, characteristic for low amylose starch types showing low gelling retrogradation capacity.

Microwave treatment induced changes in pasting properties that were dependent on the starch source, with the most pronounced modification observed in potato starch. Its pasting profile shifted from a very high and well-defined peak of viscosity followed by a marked breakdown to a continuous increase in viscosity throughout the test, with no defined peak and a complete absence of breakdown (Fig. 4F). PV dropped from 12,614 to 7879 mPa s, while peak time increased from 2.7 to 7.5 min, and pasting temperature rose from 66.1 to 71.4 °C, indicating delayed and reduced swelling. These functional changes were accompanied by the disappearance of BV (from 10,831 to 0 mPa s), a substantial increase in FV (from 3936 to 15,059 mPa s), and consequently, a marked increase in SV. Given that molecular weight and amylopectin chain-length distributions remained largely unchanged at the molecular level, the observed functional alterations are more likely associated with structural rearrangements at higher organisational levels, such as changes in amylose–amylopectin interactions or granule-derived supramolecular architecture. Previous molecular analysis demonstrated the high susceptibility of potato starch to microwave-induced rearrangements, which promote the formation of high-molecular-mass aggregates without requiring substantial changes in primary chain-length distributions (Mauro et al., 2025).

Although microwave treatment affected the pasting profiles differently depending on starch molecular and supramolecular features associated with each source, all treated starches consistently exhibited an increase in pasting temperature of 1–7 °C compared with their untreated counterparts. This behaviour, commonly reported after microwave modification of starch-based systems, has been attributed to structural rearrangements within the granules, including the formation of cross-linkages that limit granule swelling, resulting in greater temperature required to initiate granule disruption and paste formation (Vicente et al., 2026; Vicente, Mauro, et al., 2025).

Tapioca starch presented significant modification, although to a much lesser extent than potato. The PV remained unchanged but occurred at a longer time, while the TV increased markedly (from 1417 to 2722 mPa s) and the SV decreased sharply (from 2149 to 975 mPa s). Structurally, the greater proportion of chains with similar length than long amylopectin chains, possibly originating from amylose fragmentation, may have slightly delayed peak viscosity development and stabilised the system during high-temperature phases, thereby reducing viscosity fluctuations after granule rupture (Cai et al., 2024; Wei et al., 2025).

Wheat starch showed little variation of the pasting profile, the only significant changes being the 7 °C increase pasting temperature and the 33% reduction in BV. Wheat starch displayed resistance to microwave-induced modification, although small structural changes, particularly the partial hydrolysis of very long amylose chains and the subsequent increase in B-chain content, may have contributed to enhanced molecular stabilisation and viscoelastic behaviour.

The cereal starches showed moderate to low modifications in their pasting profiles after microwave treatment. Among them, the most pronounced change was observed for normal maize starch, where the TV increased notably (from 1602 to 2223 mPa s) and the BV decreased (from 1664 to 841 mPa s), suggesting improved stability and resistance to shear during heating. Structurally, these effects were accompanied by a reduction in B3 chains and a corresponding increase in B2 chains, modest changes that nevertheless enhanced the thermal stability of the starch gel. Normal rice starch exhibited only minor changes in pasting behaviour, with a significant increase only in peak time (from 6.6 to 7.0 min). Despite the limited variation in pasting parameters, Fig. 4A reveals reduced viscosity fluctuations during temperature transitions. This stabilisation may be attributed to a decrease in B3 chains and increases in A and B1 chains, along with potential structural reorganisation induced by the treatment. A similar, though milder, trend was observed in waxy rice starch (Fig. 3B). In waxy maize starch, both PV and BV decreased significantly (from 4266 to 3654 mPa s and from 2909 to 2101 mPa s, respectively). The absence of any protective effect of amylose, combined with the marked increase in short-chain amylopectin, likely contributed to the reduced swelling capacity observed in this sample.

3.5. Rheological properties of starch gels

Dynamic oscillatory tests, including strain and frequency sweeps, were carried out on 10% (w/w) gels prepared from native starches by RVA. The parameters derived from strain and frequency sweeps are summarised in Table 5, while the evolution of the elastic and viscous moduli with strain and frequency is shown in Figs. 5 and 6, respectively.

Potato and tapioca gels exhibited low consistency, with low G_1' (54 and 18 Pa, respectively) and G_1'' (22 and 10 Pa, respectively) values with moderate dependence on frequency, and relatively high $\tan\delta_1$ (0.407 and 0.555, respectively), indicating a weaker viscoelastic behaviour compared with most of the other starch gels. Both gels showed very high CPstrain values (2697% and 2819%, respectively), suggesting high deformability. However, the loss of the linear viscoelastic region occurred at much lower strain levels (MaxStrain of 27% for both samples), revealing that these gels lost structural integrity well before reaching the crossover point. This apparent extensibility therefore reflects delayed dominance of the viscous component rather than true elasticity. In potato starch, the high phosphate content and open granular structure promote molecular repulsion and allow greater deformation, conferring flexibility but limiting network reinforcement (Zhou et al., 2024). In tapioca, the presence of long amylose chains and balanced proportion of B1 and B2 chains likely hindered the initial network ordering, weakening structural integrity despite evidence of retrogradation.

Waxy maize showed weak gels, similar to those of potato and tapioca in terms of G_1' (9 Pa) and G_1'' (6 Pa) with moderate frequency dependence and relatively high $\tan\delta_1$ (0.674). It also presented low tolerance to deformation, with MaxStrain of 52%, corresponding to an MaxStress of only 5 Pa. Waxy rice starch also showed a weak gel, though to a lesser extent than maize, showing a G_1' of 216 and the same MaxStrain of 52%, but corresponding to a MaxStress of 100 Pa. This poor gelling is explained by the low amylose content, and aligns with RVA results, particularly for waxy maize that showed high breakdown, indicative of thermal instability, and low setback, reflecting poor gelling-based structural reorganisation upon cooling.

Normal maize and wheat formed the stronger and more elastic networks, with high G_1' values (1297 and 1449 Pa, respectively) with low frequency dependence (a value of −0.004 and −0.049, respectively), very low tan δ_1 (0.033 and 0.048, respectively), and high resistance to deformation (MaxStrain of 101%). This behaviour is consistent with their higher amylose content (Table 2), as leached amylose has shown to form more effective entanglements that enhance network elasticity and gel strength (Cheng et al., 2024).

Following microwave treatment, distinct rheological responses were observed across starches. Wheat and normal maize exhibited similar trends, characterised by moderate increases in consistency and decreased resistance to deformation. In both cases, G_1' increased slightly (wheat: from 1449 to 1631 Pa; maize: from 1417 to 1582 Pa), and tan δ_1 decreased (wheat: from 0.048 to 0.043; maize: from 0.043 to 0.037), indicating the formation of more elastic and structured gels. However, both MaxStress and MaxStrain declined (wheat: from 1618 to 1262 Pa and from 101 to 72%; maize: from 1519 to 1221 Pa and from 95 to 68%, respectively), reflecting reduced ability to sustain large deformations despite enhanced consistency. These changes may be attributed to the high amylose content and the generation of short linear dextrins during treatment, which likely promoted denser and more rigid gel networks (H. Li, Li, et al., 2020).

Potato gels showed marked structural reinforcement after treatment. G_1' and G_1'' increased substantially (from 54 to 1024 Pa, and from 22 to 167 Pa, respectively), while their dependence with frequency (a and b values) and $\tan\delta_1$ dropped sharply (from 0.407 to 0.163), strongly reinforcing the elastic character of the gel. MaxStress increased from 15 to 744 Pa and MaxStrain from 27 to 72%, while CPstrain dropped markedly (from 2697 to 242%), indicating enhanced cohesion. These improvements were accompanied by complete elimination of

Table 5
Parameters derived from oscillatory rheology on 10 g/100 g gels of untreated and microwave-treated starches.

Starch		CPstress	CPstrain	MaxStress	MaxStrain	G_1'	a	G_1''	b	$\tan\delta_1$	c
Normal Rice	U	254 ± 2^{a}	271 ± 4^{a}	113 ± 4^{a}	37 ± 1^{c}	308 ± 16^{a}	0.068 ± 0.005^{c}	30 ± 1^{bcd}	0.360 ± 0.002^{d}	0.098 ± 0.005^{bc}	0.292 ± 0.003^{f}
	T	232 ± 21^{a}	231 ± 35^{a}	96 ± 5^{a}	27 ± 1^{b}	370 ± 22^{a}	0.061 ± 0.001^{c}	33 ± 2^{cd}	0.352 ± 0.002^{d}	0.090 ± 0.001^{b}	0.291 ± 0.003^{f}
Waxy Rice	U	203 ± 2^{a}	242 ± 1^{a}	100 ± 1^{a}	52 ± 1^{d}	216 ± 3^{a}	0.091 ± 0.003^{d}	26 ± 1^{abcd}	0.335 ± 0.001^{cd}	0.120 ± 0.002^{cd}	0.245 ± 0.004^{e}
	T	176 ± 1^{a}	258 ± 1^{a}	79 ± 1^{a}	52 ± 1^{d}	171 ± 1^{a}	0.105 ± 0.004^{d}	25 ± 1^{abcd}	0.324 ± 0.001^{cd}	0.144 ± 0.004^{de}	0.219 ± 0.004^{d}
Normal Maize	U	1314 ± 16^{cd}	191 ± 23^{a}	1259 ± 76^{c}	101 ± 1^{f}	1297 ± 257^{bc}	-0.004 ± 0.001^{b}	43 ± 8^{d}	0.277 ± 0.001^{bc}	0.033 ± 0.001^{a}	0.281 ± 0.002^{f}
	T	1552 ± 300^{de}	162 ± 6^{a}	1272 ± 251^{c}	52 ± 1^{d}	2555 ± 475^{d}	-0.010 ± 0.005^{b}	69 ± 15^{e}	0.230 ± 0.004^{ab}	0.027 ± 0.001^{a}	0.240 ± 0.001^{e}
Waxy Maize	U	54 ± 14^{a}	638 ± 151^{b}	5 ± 1^{a}	52 ± 1^{d}	9 ± 1^{a}	0.323 ± 0.006^{g}	6 ± 1^{a}	0.493 ± 0.002^{e}	0.674 ± 0.008^{j}	0.170 ± 0.007^{c}
	T	58 ± 3^{a}	660 ± 1^{b}	3 ± 1^{a}	27 ± 1^{b}	10 ± 1^{a}	0.306 ± 0.002^{g}	6 ± 1^{a}	0.473 ± 0.009^{e}	0.619 ± 0.013^{i}	0.167 ± 0.01^{c}
Wheat	U	1679 ± 63^{e}	238 ± 17^{a}	1618 ± 4^{d}	101 ± 1^{f}	1449 ± 103^{bc}	-0.049 ± 0.006^{a}	69 ± 2^{e}	0.208 ± 0.005^{ab}	0.048 ± 0.002^{a}	0.257 ± 0.01^{e}
	T	1818 ± 70^{e}	227 ± 6^{a}	1262 ± 18^{c}	72 ± 1^{e}	1631 ± 95^{c}	-0.044 ± 0.004^{a}	71 ± 4^{e}	0.212 ± 0.001^{ab}	0.043 ± 0.001^{a}	0.257 ± 0.004^{e}
Potato	U	713 ± 59^{b}	2697 ± 127^{d}	15 ± 1^{a}	27 ± 1^{b}	54 ± 3^{a}	0.240 ± 0.008^{f}	22 ± 1^{abc}	0.369 ± 0.01^{d}	0.407 ± 0.017^{g}	0.129 ± 0.002^{b}
	T	992 ± 45^{bc}	242 ± 7^{a}	744 ± 57^{b}	72 ± 1^{e}	1024 ± 57^{b}	0.092 ± 0.003^{d}	167 ± 6^{f}	0.163 ± 0.002^{a}	0.163 ± 0.003^{e}	0.071 ± 0.005^{a}
Tapioca	U	811 ± 41^{b}	2819 ± 92^{d}	5 ± 1^{a}	27 ± 1^{b}	18 ± 1^{a}	0.305 ± 0.008^{g}	10 ± 1^{ab}	0.457 ± 0.003^{e}	0.555 ± 0.001^{h}	0.152 ± 0.006^{c}
	T	683 ± 11^{b}	1968 ± 13^{c}	8 ± 1^{a}	14 ± 1^{a}	56 ± 2^{a}	0.218 ± 0.009^{e}	20 ± 1^{abc}	0.305 ± 0.068^{cd}	0.359 ± 0.011^{f}	0.131 ± 0.001^{b}

Values are expressed as mean ± standard deviation. Different letters indicate significantly different means (Tukey's test, $\alpha = 0.05$). U = untreated starch; T = microwave-treated starch; CPstress = Crossing point stress (Pa); CPstrain = Crossing point strain (%); MaxStress = Maximum stress within the linear viscoelastic region (Pa); MaxStrain = Maximum strain within the linear viscoelastic region (%); G_1' = fitted elastic modulus at 1Hz (Pa); G_1'' = fitted viscous modulus at 1Hz (Pa); tan δ_1 = fitted loss tangent at 1 Hz; a,b,c = coefficients describing the frequency dependence of the dynamic moduli and loss tangent, respectively.

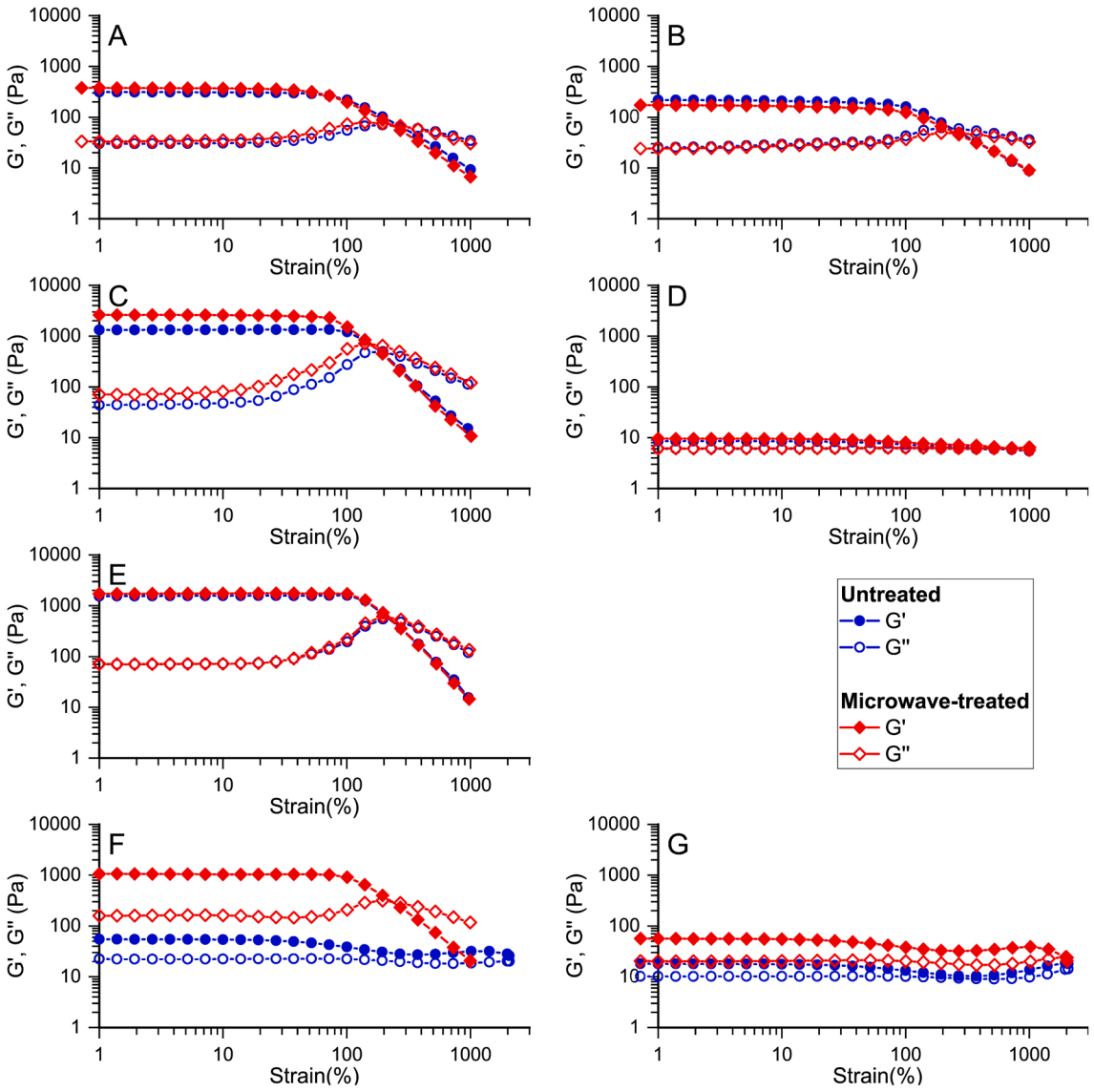

Fig. 5. Deformation sweeps in oscillatory rheology tests of 10 g/100 g gels of untreated and microwave-treated starches. (A) normal rice, (B) waxy rice, (C) normal maize, (D) waxy maize, (E) wheat, (F) potato, (G) tapioca. G': elastic modulus, G'': viscous modulus.

breakdown (0 mPa s) and a dramatic increase in setback (2153 to 7180 mPa s) in pasting characteristics, suggesting more controlled gelatinisation and enhanced amylose retrogradation. The fine structure of amylopectin, as assessed by HPAEC/PAD, showed no significant changes, supporting the hypothesis that the improved rheological performance is primarily due to physical or conformational modifications rather than changes in amylopectin fine structure.

In tapioca, although G_1' and G_1'' increased after treatment, these changes were not statistically significant. The decrease in $\tan\delta_1$ (from 0.555 to 0.359) suggested a modest enhancement in elasticity. However, reductions in CPstrain (from 2819 to 1968%) and MaxStrain (from 27 to 14%) indicate a more fragile network with lower deformation tolerance. A slight reduction in amylose, in favour of short chains resembling those of amylopectin, may have reduced the viscous character and extensibility of the gel.

Normal and waxy rice starches exhibited some similarities in their structural response to microwave treatment, with increased proportions of A and B1 chains in HPAEC/PAD chain length profiles (normal rice: from 4.4 to 6.5%; waxy rice: from 4.1 to 6.8%), suggesting fragmentation of longer chains. Nevertheless, modifications in rheological behaviour differed. Normal rice showed slight, non-significant, tendency of increase in G_1' (from 308 to 370 Pa) and decrease in $\tan\delta_1$ (from 0.098 to 0.090), suggesting marginal improvement in elasticity and consistency, as seen in other non-waxy cereals. Conversely, waxy rice exhibited slight, non-significant reduction in G_1' (from 216 to 171 Pa) and increase $\tan\delta_1$ (from 0.120 to 0.144), reflecting marginal reduction of the viscoelastic behaviour and consistency of the gels. Although both starches experienced comparable amylopectin fragmentation, the amylose present in normal rice likely promoted intermolecular reassociation and network reinforcement, while in waxy rice, the lack of amylose and predominance of short dextrins prevented effective reorganisation, leading to weaker gels. Waxy maize starch displayed minimal changes following treatment, with a slight non-significant reduction in most rheological parameters, reflecting similar mechanisms as observed in waxy rice.

3.6. Correlations between molecular and functional properties

Pearson's correlation coefficients between molecular structure parameters and pasting and rheological properties are shown in Fig. 7.

The proportions of short (AM1) and medium (AM2) amylose chains exhibited negative correlations with peak viscosity (PV). Among the

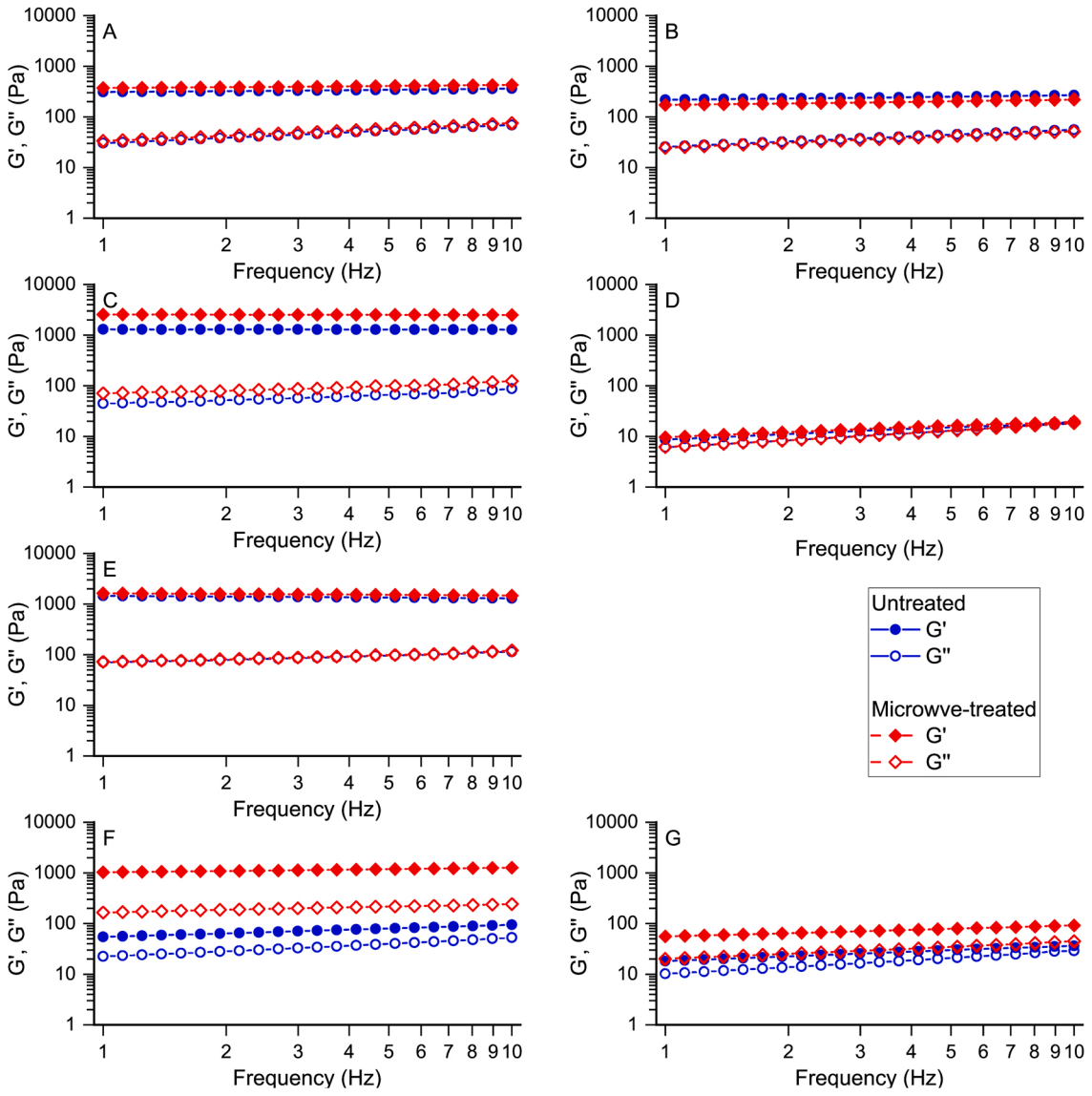

Fig. 6. Frequency sweeps in oscillatory rheology tests of 10 g/100 g gels of untreated and microwave-treated starches. (A) normal rice, (B) waxy rice, (C) normal maize, (D) waxy maize, (E) wheat, (F) potato, (G) tapioca. G': elastic modulus, G'': viscous modulus.

analysed samples, non-waxy cereal starches exhibited higher proportions of amylose chains (AM1, AM2) and lower PV values, while waxy samples showed the opposite trend. This observation supports previous research (Q. Li, Li, et al., 2020), suggesting that elevated levels of these chains diminish the swelling capacity of starch granules during pasting. Additionally, AM1 correlated negatively with BV, indicating that a greater abundance of short amylose chains may prevent a pronounced viscosity drop following granule rupture. Both AM1 and AM2 correlated positively with the Ptemp and Ptime, at which peak viscosity occurred, reflecting a greater thermal resistance to swelling in samples with higher amylose content. This is consistent with the behaviour observed in starches with higher amylose content, such as wheat and normal maize, which showed elevated Ptemp. Moreover, the chain-length at the maximum of the amylose-related peak determined by SEC/MALS-dRI-Visco (AMpeak) was positively associated with viscosities obtained in the pasting profile (PV, BV, FV, and SV), suggesting that longer amylose chains contribute to the formation of more rigid gel networks. This aligns with the increased final viscosity observed in samples with high AMpeak such as normal maize and wheat. The strongest positive correlations were found between AM1 and AM2 contents and both the fitted elastic modulus at 1 Hz (G_1') and the maximum stress within the linear viscoelastic region (MaxStress), indicating that these chains play a key role in strengthening the gel network. Similarly, total amylose content (AMT) correlated positively with both G_1' and G_1'', and negatively with $\tan\delta_1$, confirming that samples with higher amylose levels exhibit higher consistency and a more elastic behaviour. In addition, there was a strong positive correlation between amylose contents (AMT, AM1, AM2, and AM3) and gel resistance to deformation within the linear viscoelastic region (MaxStress) and stress at the crossover point (CPStress). This suggest that amylose facilitate the formation of gels that can tolerate higher degree of stress before failure.

Regarding amylopectin chains, the shortest fraction (AP1) showed negative correlations with SV, Ptime, and particularly with gel viscoelastic properties such as G_1', G_1'' and CPStress. This indicates that a predominance of very short chains hinders the development of a strong gel network. Additionally, AP1 correlated positively with $\tan\delta_1$, suggesting an increased predominance of the viscous component in relation with the elastic one. Conversely, AP2 chains were positively correlated with PV, BV, FV and SV, suggesting that these chains enhance granule swelling and viscosity development. However, their negative correlations with G_1', CPStress and MaxStrain imply that this increase in viscosity may not translate into a mechanically stronger gel network. A

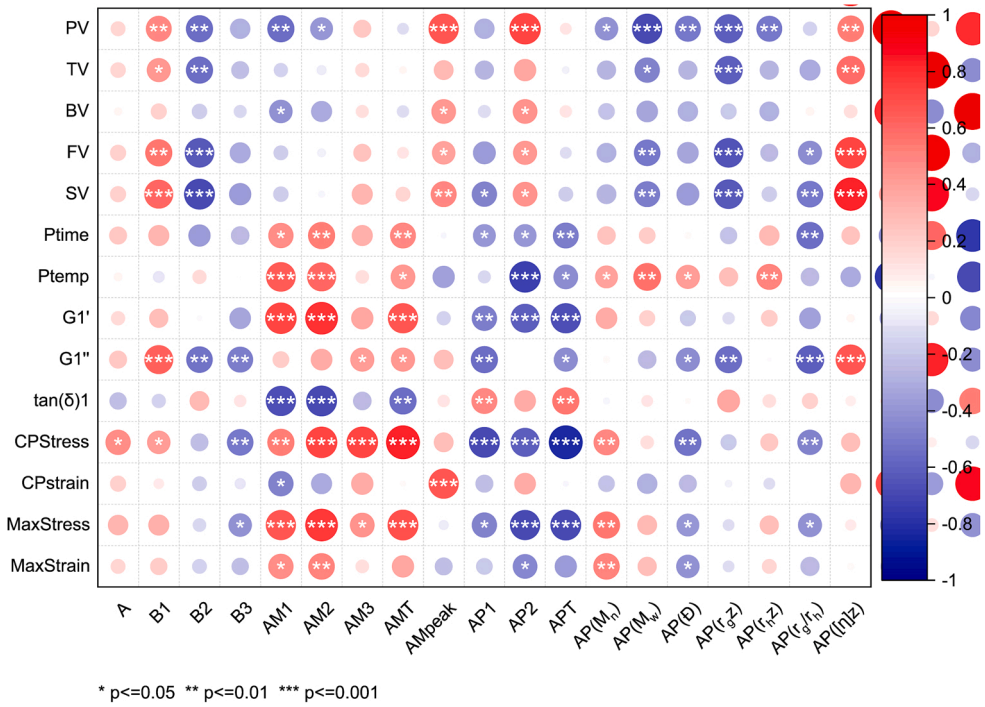

Fig. 7. Pearson correlation matrix between amylose and amylopectin molecular features and pasting and rheological parameters.

weak positive correlation was observed between the percentage of A chains and CPstress, an effect most evident in wheat starch. This starch is known to exhibit a more compact molecular structure (Mauro et al., 2025), characterised by shorter and less flexible amylopectin branches. Such structural features likely require the application of higher stress to reach the crossover point, as the network resists deformation more effectively. On the other hand, B1-type chains were positively associated with PV, FV, SV, and G_1'', indicating that these shorter chains favour viscosity development (Zhang et al., 2020). In contrast, B2 chains (intermediate branches) were negatively correlated with PV, TV, FV, SV and G_1'', suggesting that highly branched structures may reduce the viscosity of gel networks.

Parameters describing the molecular mass and size of whole amylopectin molecules showed clear relationships with pasting and viscoelastic behaviour. The number-average (M_n) and weight-average (M_w) molecular weights correlated negatively with PV and positively with Ptemp, more markedly for M_w, suggesting that larger amylopectin molecules swell less readily and require more energy to start pasting (higher PT). M_n also correlated positively with CPStress, CPStrain and MaxStrain, indicating that gels containing amylopectin molecules of higher average molecular weight withstand greater deformation and stress before network irreversible breakdown. Amylopectin molecular dispersity (Đ) was negatively correlated with PV, G_1'', CPStress, MaxStress and MaxStrain, suggesting that the presence of molecules with greater heterogeneity in molecular weight reduces peak viscosity and leads to less viscous and weaker gels. The radius of gyration (R_{gZ}) exhibited a correlation pattern similar to M_w with PV, TV, FV, SV and G_1'', which is expected given that larger molecules tend to have greater mass. The hydrodynamic radius (R_{hZ}) correlated negatively with PV and positively with Ptemp, further supporting the notion that larger molecules have reduced swelling capacity and require more energy to initiate pasting. The R_g/R_h ratio correlated negatively with FV, SV, Ptime, G_1'', CPStress, and MaxStress. This implies that more branched or less compact molecules, reflected in higher R_g/R_h values, have greater interaction with water, requiring less energy to start pasting, and developing lower viscosity. That also led to gels with lower consistency and reduced resistance to deformation. Finally, intrinsic viscosity ([η]) showed positive correlations with PV, TV, FV, SV and G_1''. This suggests that amylopectin molecules with higher intrinsic viscosities promote a greater rise in viscosity during pasting, which is maintained after granule rupture and during cooling, contributing to a more viscous gel.

3.7. Principal components analysis

Principal Components Analysis (PCA) revealed a clear segregation of structural and functional variables across four quadrants defined by PC1 and PC2, which together accounted for 60.55% of the total variance (Fig. 8). In the upper right quadrant (positive PC1 and PC2 values), samples clustered with pasting parameters Ptemp and Ptime, rheological indicators such as MaxStrain, MaxStress and CPStress, amylose-derived fractions (AM1, AM2, AMT), and whole amylopectin parameters (AP(R_h), AP[η]). This quadrant included non-waxy cereal starches such as wheat and normal maize. These samples were characterised by amylopectin molecules with large hydrodynamic radii and high molecular dispersity (as determined by SEC), combined with elevated amylose contents. This structural profile likely hindered granule swelling during pasting, requiring more energy and longer times to reach peak viscosity. Their gels exhibited more elastic behaviour and greater resistance to deformation.

Also located in the upper half of the plot, but with negative PC1 values, were waxy maize and native normal rice, the latter positioned closer to the non-waxy cereals. This region was inversely related to high amylose parameters but still reflected high molecular mass values. These samples showed higher proportions of long amylopectin chains (B2 and B3), which likely promoted increased water interaction, leading to more fluid, less elastic gels with reduced structural strength.

In this left-side quadrant (negative PC1), elevated R_g/R_h ratios were also observed, suggesting more highly branched, less viscous structures under pasting conditions. This region was further associated with higher levels of APT, AP1, and AP2 chains, contributing to greater granule swelling capacity (higher PV) and increased viscosity breakdown (higher BV). Waxy rice, sharing a similar viscoelastic profile with waxy maize, was located in this area along with tapioca and potato starches. These latter samples were distinguished by their high CPStrain in

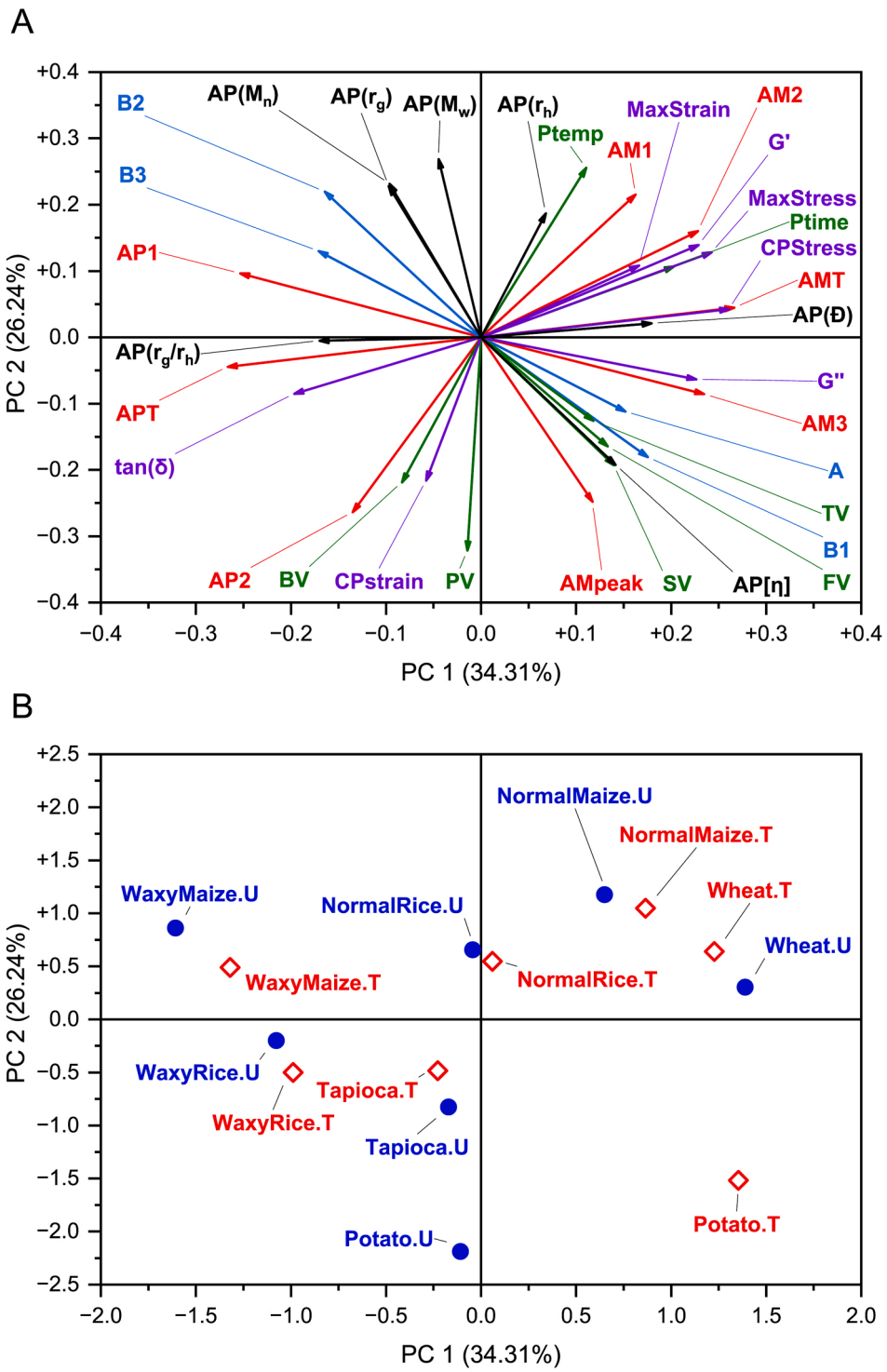

Fig. 8. Principal component analysis (PCA). (A) Loading plot showing variable distribution; (B) score plot showing sample distribution. (U) untreated and (T) microwave-treated samples.

rheological tests and pronounced peak viscosities.

Among the microwave-treated samples, three distinct patterns of change were observed in the PCA scores. Potato starch showed the most pronounced shift, with increases in both PC1 and PC2 scores, being the only sample located in the lower right quadrant. The direction of this shift reflects extensive alterations in viscoelastic properties and network structure, including the pronounced increase in G_1', G_1'', CPStress, TV, FV and SV, and reduced PV, BV, $\tan\delta_1$ and CPStrain of treated potato starch.

Tapioca and wheat starches exhibited a reduction in PC1 and an increase in PC2, but staying in the same quadrant (upper right for wheat and lower left for tapioca). In tapioca, this shift was supported by reductions in PV, BV, SV, and $\tan\delta_1$, alongside an increase in G_1' and long amylopectin chains (B2 and B3). Wheat followed a similar trend, with its changes primarily associated reduced PV, BV, CPStrain and increased CPstress, G_1', and B2 amylopectin chains.

The remaining samples (normal maize, normal rice, and the waxy starches) showed increases in PC1 and decreases in PC2 after microwave

treatment. For normal rice, this shift corresponded to a transition from the upper-left to the upper-right quadrant. For these samples, the displacement seems to be mainly related to the more molecular degradation induced by the treatment. Reductions in AP(M_n), AP(M_w), AP(r_g), AP(r_h), and B3 chains, together with increases in A and B1 chains, were common across this group and largely governed their positioning in the PCA space, particularly for waxy starches. Reductions in pasting parameters (PV, BV, FV and SV) moderated the shift. An exception was normal maize, which exhibited increased TV and FV, reinforcing its displacement towards higher PC1 and lower PC2 values.

4. Conclusion

This study provides novel insights into the structural and functional behaviour of different types of starches subjected to microwave treatment under strictly controlled temperature and moisture conditions. Using starches with contrasting molecular and supramolecular architectures, representative of cereals, roots, and tubers, allowed the identification of both general trends and structure-dependent responses.

Microwave treatment induced distinct, source-dependent responses, even among samples with similar structural features. Waxy starches exhibited marked increases in short amylopectin chains and significant reductions in molecular weight and size, particularly in waxy rice. However, these changes had limited rheological impact, likely due to the absence of amylose and the restricted capacity of the degraded amylopectin fragments to promote network reorganisation. In contrast, potato starch showed pronounced alterations in viscoelastic properties despite only minor changes in chain-length distribution, suggesting that supramolecular reorganisation due to microwave treatment, rather than chain scission, dominated its functional response. Tapioca starch exhibited higher proportion of chains with degrees of polymerisation similar to long amylopectin branches, which may explain its improved gel stability and reduced viscosity loss after pasting. Wheat and normal maize starches, both rich in amylose, displayed moderate molecular modification accompanied by enhanced gel stability, consistent with the fragmentation of long amylose chains into segments comparable in size to long amylopectin branches, which may facilitate new molecular interactions. Normal and waxy rice starches, though similar in their amylopectin chain profiles, displayed contrasting gel behaviours after treatment. While amylopectin defined viscoelastic properties, the presence or absence of amylose, in the regimes tested, modulated their response: treated normal rice resembled other non-waxy cereals, whereas waxy rice aligned more closely with waxy maize.

The absence of major differences in the SEC/MALS-dRI-Visco profiles of debranched samples contrasted with the significant changes observed in whole amylopectin molecules, suggesting that microwave-induced hydrolysis primarily targeted α(1 → 6) glycosidic linkages at branching points. However, cleavage of α(1 → 4) bonds was also evident from HPAEC/PAD analysis, which revealed the formation of short fragments resembling amylopectin short chains. In wheat and tapioca starches, the presence of long-chain amylose appeared to favour the generation of longer hydrolysis products with degrees of polymerisation comparable to long amylopectin branches.

Overall, these results emphasise that starch functional response to hydrothermal processing assisted by microwaves arises from the interplay between composition (amylose and amylopectin content), molecular architecture (chain-length distribution), and supramolecular organisation (granular structure). The controlled approach used in this study with fixed treatment conditions and use of pure starches provides a valuable scientific framework for understanding the mechanistic basis of starch behaviour under microwave radiation and guiding the design of targeted treatments to fine-tune texture and viscosity in real food systems.

Acronyms and corresponding analytical methods used in this work

Acronym	Parameter	Method
[η]	Intrinsic viscosity	SEC/MALS-dRI-Visco
A	Percentage of amylopectin A-chains (DP 6-12, %)	HPAEC/PAD
AM1	Percentage of group 1 amylose chains (DP ~100-300, %)	SEC/MALS-dRI-Visco
AM2	Percentage of group 2 amylose chains (DP > 300 - 1600, %)	SEC/MALS-dRI-Visco
AM3	Percentage of group 3 amylose chains (DP > 1600, %)	SEC/MALS-dRI-Visco
AMpeak	Glucose units of peak amylose concentration (DP)	SEC/MALS-dRI-Visco
AMT	Percentage of total amylose chains (AM1 + AM2 + AM3, %)	SEC/MALS-dRI-Visco
AP1	Percentage of short amylopectin chains (%)	SEC/MALS-dRI-Visco
AP2	Percentage of long amylopectin chains (%)	SEC/MALS-dRI-Visco
APT	Percentage of total amylopectin chains (AP1 +AP2) (%)	SEC/MALS-dRI-Visco
B1	Percentage of amylopectin B1 chains (DP 13-24, %)	HPAEC/PAD
B2	Percentage of amylopectin B2 chains (DP, 25-36, %)	HPAEC/PAD
B3	Percentage of amylopectin B3 chains (DP ≥ 37, %)	HPAEC/PAD
BV	Breakdown Viscosity (mPa·s)	RVA
CPStrain	Deformation at crossover point (%)	Rheology - strain sweep
CPStress	Stress at crossover point (Pa)	Rheology - strain sweep
FV	Final Viscosity (mPa·s)	RVA
G'	Elastic modulus (Pa)	Rheology - frequency sweep
G''	Viscous modulus (Pa)	Rheology - frequency sweep
MaxStrain	Maximum strain in the linear viscoelastic region (%)	Rheology - strain sweep
MaxStress	Maximum stress in the linear viscoelastic region (Pa)	Rheology - strain sweep
M_n	Number-average molecular weight	SEC/MALS-dRI-Visco
M_w	Weight-average molecular weight	SEC/MALS-dRI-Visco
PT	Pasting temperature (°C)	RVA
Ptime	Time to peak viscosity (min)	RVA
PV	Peak viscosity (mPa·s)	RVA
R_gz	z-average radius of gyration	SEC/MALS-dRI-Visco
R_hz	z-average hydrodynamic radius	SEC/MALS-dRI-Visco
SV	Setback Viscosity (mPa·s)	RVA
tanδ	loss tangent (G''/G')	Rheology - frequency sweep
TV	Trough viscosity (mPa·s)	RVA

CRediT authorship contribution statement

Raúl Ricardo Mauro: Writing – original draft, Methodology, Investigation, Formal analysis, Data curation, Conceptualization. **Zhihang Li:** Methodology, Investigation, Conceptualization. **Andreas Blennow:** Writing – review & editing, Visualization, Supervision, Resources, Methodology, Investigation, Data curation, Conceptualization. **Ainhoa Vicente:** Writing – review & editing, Visualization, Formal analysis. **Felicidad Ronda:** Writing – review & editing, Visualization, Supervision, Resources, Project administration, Methodology, Investigation, Funding acquisition, Data curation, Conceptualization.

Declaration of competing interest

The authors declare that they have no known competing financial interests or personal relationships that could have appeared to influence the work reported in this paper.

Acknowledgement

The authors thank the Spanish Ministerio de Ciencia e Innovación (EQC2021-006985-P), Ministerio de Ciencia, Innovación y Universidades (PID2023-153330OB-I00) and the Department of Education of the Junta de Castilla y León and FEDER Funds (Strategic Research Program CLU–2025–02–05, Institute of Bioeconomy of the University of Valladolid, BioEcoUVa) for their financial support. Raúl R. Mauro thanks the Ministry of Science, Innovation and Universities for the FPI contract.

Data availability

Data will be made available on request.

References

Bertoft, E., Annor, G. A., Shen, X., Rumpagaporn, P., Seetharaman, K., & Hamaker, B. R. (2016). Small differences in amylopectin fine structure may explain large functional differences of starch. *Carbohydrate Polymers, 140*, 113–121. https://doi.org/10.1016/J.CARBPOL.2015.12.025

Blennow, A., & Engelsen, S. B. (2010). Helix-breaking news: Fighting crystalline starch energy deposits in the cell. *Trends in Plant Science, 15*(4), 236–240. https://doi.org/10.1016/j.tplants.2010.01.009

Blennow, A., Mette Bay-Smidt, A., & Bauer, R. (2001). Amylopectin aggregation as a function of starch phosphate content studied by size exclusion chromatography and on-line refractive index and light scattering. *International Journal of Biological Macromolecules, 28*(5), 409–420. https://doi.org/10.1016/S0141-8130(01)00133-7

Calix-Rivera, C. S., Villanueva, M., Náthia-Neves, G., & Ronda, F. (2023). Changes on techno-functional, thermal, rheological, and microstructural properties of tef flours induced by microwave Radiation—Development of new improved gluten-free ingredients. *Foods, 12*(6). https://doi.org/10.3390/foods12061345

Cave, R. A., Seabrook, S. A., Gidley, M. J., & Gilbert, R. G. (2009). Characterization of starch by size-exclusion chromatography: The limitations imposed by shear scission. *Biomacromolecules, 10*(8), 2245–2253. https://doi.org/10.1021/BM900426N

Cereals & Grains Association. (2010). AACC International Method 76–21.02. General pasting method for wheat or rye flour of starch using the Rapid Visco analyser. First approval October 15, 1997; revised November 2017. In *AACC approved methods of analysis* (11th ed.). American Association of Cereal Chemists International. https://doi.org/10.1094/AACCIntMethod-76-21.01.

Chen, C., & Zhu, F. (2024). Molecular structure in relation to swelling, gelatinization, and rheological properties of lotus seed starch. *Food Hydrocolloids, 146*, Article 109259. https://doi.org/10.1016/J.FOODHYD.2023.109259

Cheng, Y., Yuqing, H., Xiao, L., Gao, W., Kang, X., Sui, J., & Cui, B. (2024). Impact of starch amylose and amylopectin on the rheological and 3D printing properties of corn starch. *International Journal of Biological Macromolecules, 278*, Article 134403. https://doi.org/10.1016/J.IJBIOMAC.2024.134403

Ding, L., Blennow, A., & Zhong, Y. (2024). Differential roles of C-3 and C-6 phosphate monoesters in affecting potato starch properties. *Grain & Oil Science and Technology, 7*(2), 79–86. https://doi.org/10.1016/J.GAOST.2024.02.001

Dobrynin, A. V., Sayko, R., & Colby, R. H. (2023). Viscosity of polymer solutions and molecular weight characterization. *ACS Macro Letters, 12*(6), 773–779. https://doi.org/10.1021/ACSMACROLETT.3C00219

Genkina, N. K., Wikman, J., Bertoft, E., & Yuryev, V. P. (2007). Effects of structural imperfection on gelatinization characteristics of amylopectin starches with A- and B-type crystallinity. *Biomacromolecules, 8*(7), 2329–2335. https://doi.org/10.1021/bm070349f

Guo, P., Li, Y., An, J., Shen, S., & Dou, H. (2019). Study on structure-function of starch by asymmetrical flow field-flow fractionation coupled with multiple detectors: A review. *Carbohydrate Polymers, 226*, Article 115330. https://doi.org/10.1016/J.CARBPOL.2019.115330

Haydukivska, K., Blavatska, V., & Paturej, J. (2020). Universal size ratios of Gaussian polymers with complex architecture: Radius of gyration vs hydrodynamic radius. *Scientific Reports, 10*(1), 1–11. https://doi.org/10.1038/S41598-020-70649-Z. SUBJMETA.

Hernández-Cifre, J. G., Collado-González, M., Díaz Baños, F. G., & García de la Torre, J. (2025). Size-Exclusion chromatography of macromolecules: A brief tutorial overview on fundamentals with computational tools for data analysis and determination of structural information. *Polymers, 17*(5), 582. https://doi.org/10.3390/POLYM17050582, 2025, Vol. 17, Page 582.

Huang, B., Huang, Q., Zhang, Y., He, W., Wang, K., & Yang, L. (2024). Influence of the molecular structure of amylopectin from waxy and sweet waxy corn on the properties of corn flour and the quality of sweet dumplings. *International Journal of Biological Macromolecules, 282*, Article 137204. https://doi.org/10.1016/J.IJBIOMAC.2024.137204

Kasemsuwan, T., & Jane, J.-L. (1996). Quantitative method for the survey of starch phosphate derivatives and starch phospholipids by 31P nuclear magnetic resonance spectroscopy. *Cereal Chemistry, 73*(6), 702–707.

Li, C., Wu, A., Yu, W., Hu, Y., Li, E., Zhang, C., & Liu, Q. (2020). Parameterizing starch chain-length distributions for structure-property relations. *Carbohydrate Polymers, 241*, Article 116390. https://doi.org/10.1016/J.CARBPOL.2020.116390

Li, H., Li, J., & Guo, L. (2020). Rheological and pasting characteristics of wheat starch modified with sequential triple enzymes. *Carbohydrate Polymers, 230*, Article 115667. https://doi.org/10.1016/J.CARBPOL.2019.115667

Li, Q., Li, C., Li, E., Gilbert, R. G., & Xu, B. (2020). A molecular explanation of wheat starch physicochemical properties related to noodle eating quality. *Food Hydrocolloids, 108*, Article 106035. https://doi.org/10.1016/J.FOODHYD.2020.106035

Mauro, R. R., Vela, A. J., & Ronda, F. (2023). Impact of starch concentration on the pasting and rheological properties of gluten-free gels. Effects of amylose content and thermal and hydration properties. *Foods, 12*(12), 2281. https://doi.org/10.3390/foods12122281

Mauro, R. R., Vicente, A., & Ronda, F. (2025). Molecular modifications in cereal and tuber starches induced by microwave treatment: A comprehensive analysis using asymmetric flow field-flow fractionation. *International Journal of Biological Macromolecules, 316*, Article 144395. https://doi.org/10.1016/J.IJBIOMAC.2025.144395

Nygaard, M., Kragelund, B. B., Papaleo, E., & Lindorff-Larsen, K. (2017). An efficient method for estimating the hydrodynamic radius of disordered protein conformations. *Biophysical Journal, 113*(3), 550–557. https://doi.org/10.1016/J.BPJ.2017.06.042

Oyeyinka, S. A., Akinware, R. O., Bankole, A. T., Njobeh, P. B., & Kayitesi, E. (2021). Influence of microwave heating and time on functional, pasting and thermal properties of cassava starch. *International Journal of Food Science and Technology, 56*(1). https://doi.org/10.1111/ijfs.14621

Ronda, F., Pérez-Quirce, S., Angioloni, A., & Collar, C. (2013). Impact of viscous dietary fibres on the viscoelastic behaviour of gluten-free formulated rice doughs: A fundamental and empirical rheological approach. *Food Hydrocolloids, 32*(2), 252–262. https://doi.org/10.1016/j.foodhyd.2013.01.014

Tian, Y., Wang, Y., Herbuger, K., Petersen, B. L., Cui, Y., Blennow, A., Liu, X., & Zhong, Y. (2023). High-pressure pasting performance and multilevel structures of short-term microwave-treated high-amylose maize starch. *Carbohydrate Polymers, 322*. https://doi.org/10.1016/j.carbpol.2023.121366

Vela, A. J., Villanueva, M., Li, C., Hamaker, B., & Ronda, F. (2023). Ultrasound treatments of tef [Eragrostis tef (Zucc.) Trotter] flour rupture starch α-(1,4) bonds and fragment amylose with modification of gelatinization properties. *Lebensmittel-Wissenschaft und -Technologie, 174*, Article 114463. https://doi.org/10.1016/j.lwt.2023.114463

Vicente, A., Caballero, P. A., Villanueva, M., & Ronda, F. (2026). Advances in microwave-induced physical modification of flours: From structural changes to product development. *Food Hydrocolloids, 172*, Article 112026. https://doi.org/10.1016/J.FOODHYD.2025.112026

Vicente, A., Mauro, R. R., Villanueva, M., Caballero, P. A., Hamaker, B., & Ronda, F. (2025). Molecular and structural changes in starch and proteins induced by microwave treatment and their effect on pasting properties. A study on amaranth, buckwheat, quinoa, and sorghum in grain and flour form. *International Journal of Biological Macromolecules, 318*, Article 145094. https://doi.org/10.1016/J.IJBIOMAC.2025.145094

Vicente, A., Villanueva, M., Muñoz, J. M., Caballero, P. A., & Ronda, F. (2025). The role of microwave absorption capacity and water mobility in the microwave treatment of grain vs. flour: Impact on the treated flour characteristics. *Food Hydrocolloids, 159*, Article 110680. https://doi.org/10.1016/J.FOODHYD.2024.110680

Viksø-Nielsen, A., Blennow, A., Jørgensen, K., Kristensen, K. H., Jensen, A., & Møller, B. L. (2001). Structural, physicochemical, and pasting properties of starches from potato plants with repressed r1-Gene. *Biomacromolecules, 2*(3), 836–843. https://doi.org/10.1021/BM0155165

Wang, Y., Tian, Y., Li, Z., Kirkensgaard, J. J. K., Svensson, B., & Blennow, A. (2024). Interfacial kinetics reveal enzymatic resistance mechanisms behind granular starch with smooth surfaces. *Food Bioscience, 60*, Article 104448. https://doi.org/10.1016/J.FBIO.2024.104448

Wei, Y., Li, G., & Zhu, F. (2025). Microwave-Induced structural and functional changes in small granule starch. *Food and Bioprocess Technology, 18*(7), 6213–6227. https://doi.org/10.1007/S11947-025-03802-Z/FIGURES/5

Wong, K. S., & Jane, J. (1995). Effects of pushing agents on the separation and detection of debranched amylopectin by high-performance anion-exchange chromatography with pulsed amperometric detection. *Journal of Liquid Chromatography, 18*(1), 63–80. https://doi.org/10.1080/10826079508009221

Xu, F., Zhang, L., Liu, W., Liu, Q., Wang, F., Zhang, H., Hu, H., & Blecker, C. (2021). Physicochemical and structural characterization of potato starch with different degrees of gelatinization. *Foods, 10*(5), 1104. https://doi.org/10.3390/FOODS10051104/S1

Yang, L., Liu, Y., Wang, S., Zhang, X., Yang, J., & Du, C. (2021). The relationship between amylopectin fine structure and the physicochemical properties of starch during potato growth. *International Journal of Biological Macromolecules, 182*, 1047–1055. https://doi.org/10.1016/J.IJBIOMAC.2021.04.080

Yang, Q., Qi, L., Luo, Z., Kong, X., Xiao, Z., Wang, P., & Peng, X. (2017). Effect of microwave irradiation on internal molecular structure and physical properties of waxy maize starch. *Food Hydrocolloids, 69*, 473–482. https://doi.org/10.1016/j.foodhyd.2017.03.011

Zhang, Z., Li, E., Fan, X., Yang, C., Ma, H., & Gilbert, R. G. (2020). The effects of the chain-length distributions of starch molecules on rheological and thermal properties of wheat flour paste. *Food Hydrocolloids, 101*, Article 105563. https://doi.org/10.1016/J.FOODHYD.2019.105563

Zhao, X., Hofvander, P., Andersson, M., & Andersson, R. (2023). Internal structure and thermal properties of potato starches varying widely in amylose content. *Food Hydrocolloids, 135*, Article 108148. https://doi.org/10.1016/J.FOODHYD.2022.108148

Zhao, Y., Tu, D., Wang, D., Xu, J., Zhuang, W., Wu, F., & Tian, Y. (2024). Structural and property changes of starch derivatives under microwave field: A review. *International Journal of Biological Macromolecules, 256*, Article 128465. https://doi.org/10.1016/J.IJBIOMAC.2023.128465

Zheng, L., Zhang, Q., Yu, X., Luo, X., & Jiang, H. (2023). Effect of annealing and heat-moisture pretreatment on the quality of 3D-printed wheat starch gels. *Innovative Food Science & Emerging Technologies, 84*, Article 103274. https://doi.org/10.1016/J.IFSET.2023.103274

Zhong, Y., Xiang, X., Chen, T., Zou, P., Liu, Y., Ye, J., Luo, S., Wu, J., & Liu, C. (2020). Accelerated aging of rice by controlled microwave treatment. *Food Chemistry, 323*, Article 126853. https://doi.org/10.1016/J.FOODCHEM.2020.126853

Zhong, Y., Xiang, X., Zhao, J., Wang, X., Chen, R., Xu, J., Luo, S., Wu, J., & Liu, C. (2020). Microwave pretreatment promotes the annealing modification of rice starch. *Food Chemistry, 304*, Article 125432. https://doi.org/10.1016/J.FOODCHEM.2019.125432

Zhou, T., Zhang, Y., Wang, Y., Liu, Q., Yang, Y., Qiu, C., Jiao, A., & Jin, Z. (2024). Impact of freeze-thaw cycles on the physicochemical properties and structure-function relationship of potato starch with varying granule sizes in frozen dough. *International Journal of Biological Macromolecules, 279*, Article 134864. https://doi.org/10.1016/J.IJBIOMAC.2024.134864